Copyright Warning & Restrictions

The copyright law of the United States (Title 17, United States Code) governs the making of photocopies or other reproductions of copyrighted material.

Under certain conditions specified in the law, libraries and archives are authorized to furnish a photocopy or other reproduction. One of these specified conditions is that the photocopy or reproduction is not to be "used for any purpose other than private study, scholarship, or research." If a, user makes a request for, or later uses, a photocopy or reproduction for purposes in excess of "fair use" that user may be liable for copyright infringement,

This institution reserves the right to refuse to accept a copying order if, in its judgment, fulfillment of the order would involve violation of copyright law.

Please Note: The author retains the copyright while the New Jersey Institute of Technology reserves the right to distribute this thesis or dissertation

Printing note: If you do not wish to print this page, then select "Pages from: first page # to: last page #" on the print dialog screen

ABSTRACT

VALIDATION OF A MATHEMATICAL MODEL OF THE HUMAN WALKING CYCLE USING PARAMETER IDENTIFICATION METHODS

by
Robert McCann

A mathematical model of the swing phase, toe-off and heel strike is presented in this paper and is mathematically represented as a two dimensional, simple coupled pendulum system with three degrees of freedom. Lagrange equations of motion are used to solve this highly idealized system. The model consists of three segments which represent the stance leg, thigh and shank. During the swing phase it is assumed that the only external forces acting on the system are gravity and viscous dissipative terms proportional to joint angular velocities. It is assumed that muscle forces act only to establish the initial limb segment configuration and velocities at the start of the swing and toe-off.

The mechanical energy of this system is examined to determine optimum gait parameters that minimize mechanical energy losses.

Theoretical results from this model are compared to collected experimental data obtained from clinical trials, for each experimental trial the mass and centers of mass of the limb segments is altered by attaching known fixed weights to the experimental subject. The altered gait patterns that result are recorded and compared to theoretical predictions of the model.

Numerical analysis is used to minimize the error that occurs in the model, thus verification of model and gait parameter identification is examined. Findings suggest that the model predictions agree with experimental data, however, the model is sensitive to parameter changes and finding values which minimize residual error in the model need further investigation. It is hopeful that eventually this model will be used as a clinical tool for optimizing gait mechanics and prosthetic design.

VALIDATION OF A MATHEMATICAL MODEL OF THE HUMAN WALKING CYCLE USING PARAMETER IDENTIFICATION METHODS

by
Robert McCann

A Thesis
Submitted to the Faculty of
New Jersey Institute of Technology
in Partial Fulfillment of the Requirements for the Degree of
Master of Science in Biomedical Engineering

Biomedical Engineering Commitee

May 1996

APPROVAL PAGE

VALIDATION OF A MATHEMATICAL MODEL OF THE HUMAN WALKING CYCLE USING PARAMETER IDENTIFICATION METHODS

Robert McCann

Dr. H. Michael Lacker, Theses Advisor — Date
Professor of Mathematics, NJIT

Dr. Peter Engler, Theses Co-Advisor — Date
Assistant Chairperson, Graduate Advisor, and Associate Professor of Electrical Engineering, NJIT

Dr. David Kristol, Committee Member — Date
Director and Graduate Advisor of Biomedical Engineering, Professor of Chemistry, NJIT

BIOGRAPHICAL SKETCH

Author: Robert McCann

Degree: Master of Science

Date: May 1996

Undergraduate and Graduate Education:

- Master of Science in Biomedical Engineering
  New Jersey Institute of Technology, Newark, NJ, 1996

- Master of Science in Mechanical Engineering
  New Jersey Institute of Technology, Newark, NJ, 1992

- Bachelor of Science in Engineering Technology
  New Jersey Institute of Technology, Newark, NJ, 1989

Major: Biomedical Engineering

This thesis is dedicated in
Memory of the late Robert McCann Sr., 1931-1995

ACKNOWLEDGMENT

The author wishes to express his sincere gratitude to his supervisor, Dr. H. Michael Lacker, for his guidance and moral support throughout this research.

Special thanks to Professor Peter Engler for serving as theses co-advisor and Dr. David Kristol for serving as a committee member.

The author would also like to thank the Motion Analysis Group at Kessler Institute of Rehabilitation, West Orange, New Jersey, and the electrical engineering lab at the Veterans Administration Hospital, East Orange, New Jersey. This work could not have been made possible without the use of their equipment and each individuals willingness to help.

TABLE OF CONTENTS

LIST OF FIGURES

LIST OF TABLES

CHAPTER 1

INTRODUCTION

A simple mathematical model is proposed for determination of gait parameter values based on computation of the Lagrange equations of motion. These equations describe a three degree of freedom coupled pendulum system that models the swing phase of the walk cycle. The Lagrange equations of motion are second order and non-linear and will be discussed throughout this paper. They are presented along with the model in chapter 4. Computer algorithms are used to solve the motion equations that represent the model. Experimental data is collected for determination of eleven anthropometric (body segment) parameters. These model parameter values define a model individual's structure and include segment mass, center of mass and joint viscosity coefficients. Many of these parameters were originally obtained from Dempster's data on cadavers. This data is listed in appendix A.

During the swing phase the body is represented as three segments or links, one being the stance leg, and two for the thigh and shank. The swing leg and upper body are assumed to move through the swing cycle under the effects of gravity but without any additional muscular effort beyond that required for establishing the initial configuration and velocity of these segments at the beginning of the swing phase. This principle was used in the early works of human motion by Weber(2), who claimed that during the swing phase of walking, muscular control was not necessary, and the motion of the swing leg behaved much like that of a simple pendulum system acting under gravity alone. In fact, our model from a mechanical point of view, is similarly represented as a lumped mass pendulum system during the swing phase.

Our modeling efforts build upon the earlier work of Mochon and McMahon(1) and Hatze(19). As in Hatze, our model includes energy dissipation terms derived from impulsive impact forces (for example, at heel contact and full knee extension). The model

of Mochon and McMahon(1) conserves mechanical energy during the swing phase.They use Dempster's data on cadavers for identification of anthropometric parameters.

As in the earlier work of Lacker(9) we have preserved the characteristics of the original Mochon and McMahon swing phase model by starting with a 2-D, straight-stance leg, 3-coupled pendulum system. (Hatze's model is somewhat unwieldy requiring 247 input parameters!). Lacker has also added a double support phase to Mochon and McMahon's swing phase model and therefore obtains solutions for the complete walking cycles in a non-conservative system. Energy losses arise both due to collisions (heel strike, full knee extension) and velocity dependent dissipation (joint viscosity). Energy sources due to muscular effort are also included (implicitly) in the model at the begining of each walking phase (toe-off and heal-strike) where solutions are continuous but have discontinuous derivatives.

For a given individual (set of anthropometric parameters), each walk (model solution) is assigned in the model a mechanical energy efficiency (mechanical energy loss/walking distance) and a stability index that reflects the degree of neuromuscular control required to achieve that walk. Figure 1 illustrates a typical time cycle of each walking phase. The model generates an ensemble of walking solutions consistent with any given set of anthropometric parameters (model individual). For such an individual (in the three-link model system) a given walk in the ensemble of solutions is fixed by a choice of 4 independent parameters (walking speed, step length, fraction of cycle in swing phase and the toe-off angle at the time of swing initiation). These gait parameters are obtained directly from the experimental records. In this paper a method for identifying the anthropometric parameters (segment masses, centers of mass and joint viscosity coeficients) from walks of experimental subjects is examined and compared to parameters obtained from Dempster's data on cadavers. Theoretical predictions of an individual's structural parameters can be obtained by searching for those model parameter values that

minimize the (least square) error between theoretical solution (joint angle) curves and experimental data curves. Theoretical predictions are compared to experimental data. The notion of optimal gait parameters that minimize mechanical energy loss per unit distance is also discussed.

Over the past century much work has been devoted to the analysis of human walking, but few seldom discuss parameter identification, in order to minimize mechanical energy expenditure. At this time, however, these energy considerations will be considered to be secondary since the main goal of this study is structural parameter identification based on the curve fitting described above .

Within the past 40 years that work in metabolic energy expenditure and gait parameter variability has been explored empirically by such researchers as Inman (3), Nubar and Contini(4), similarly by comparison relatively few theoretical approaches have been made to analyze mechanical energy and its loss at different phases of human gait.

Theoretical results are compared to experimental results with the goal of gradually developing a model that is sufficient for understanding, interpreting and modifying gait parameters in the physically disabled.

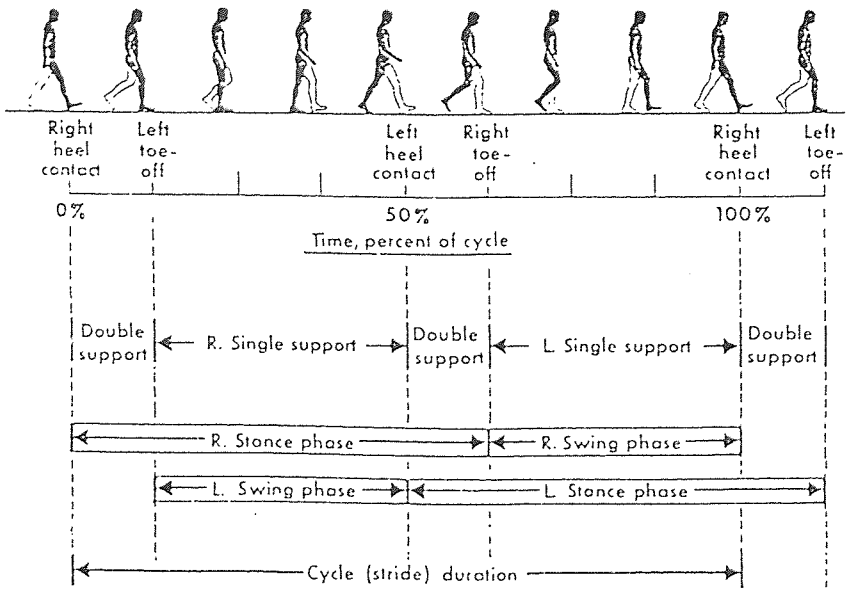

Figure 1. Distance and Time Dimensions of Walking Cycle

CHAPTER 2

LITERATURE SURVEY

2.1 Previous Research

2.1.1 Feedback

The human skeletal system is connected together by an intricate system of ligaments, tendons and muscles; this gives the structural support that is necessary for the human body to perform daily functions such as walking. With the help of muscular actions, the human body can perform a multitude of coordinated limb movements by the use of its many articulating joints. Walking, as simple as it may appear, is controlled by a complex nuero-muscular feedback system which regulates joint motion and associated muscle contraction, which initiates response enabling human motion. The human brain is the control system initiating and receiving feedback that is monitoring joint and segment position, action potentials that cause muscle contraction, resulting in forces at articulating joints. This sequence of events with coordination and motor skill produce human walking. Human walking is a learned process. After many unsuccessful attempts to walk, the infant eventually develops greater stability and precision. This process develops rapidly up until the age of seven. Apparently during this period of time, the child is experimenting with their neuromusculoskeletal system, making adjustments by modifying the displacements that occur in various segments with the accompanying changes in bodily proportions and developing improved neural controls as outlined by Inman(3). This is also true of humans who are physically disabled, suffering from crippling injuries and disease, many of these individuals must try and develop neuromusculoskeletal control all over again, often with the additional burden of having damaged muscle and neuro-networks; not an easy task. Many physically challenged must compensate by learning to use other neuromusculoskeletal systems than normals to achieve desired function and stability.

2.1.2 Energy Expenditure

Walking is one of the most common human activities, the energetics have been researched in various studies. Inman(3) for example, hypothesized that the human body will integrate the motion of various segments of the body and control the activity of the muscles in order to minimize metabolic energy expenditure. His study of human motion described the translation of the center of mass through space along a path which required the least energy expenditure. His findings proved to be accurate when compared to experimental results. His hypothesis was correct, and established a basis for the further understanding of energy expenditure. Fenn(5,6), one of the early pioneers in human motion analysis, examined the changes that occur in potential and kinetic energy when a subject is walking or running which was the basis for Inman's work.

It is important to realize that the human body during a walk cycle is very dynamic, many movements occur generating a great deal of energy expenditure, depending on the level of activity. These movements are integrated and include vertical displacements, horizontal rotation of the pelvis, mediolateral pelvic tilt, plantar flexion of the ankle and foot, knee flexion, lateral displacements of the torso, and rotation of the shoulder. During these motions potential and kinetic energy is constantly changing. The motion is well coordinated so that potential and kinetic energy are transfered back and forth during walking. This natural occurrence in human walking illustrates a human's ability to minimize mechanical energy expenditure and reduce muscle work.

Seireg and Arvikar(7), did studies relating to muscular load sharing and articulating joint forces on the lower extremities. This model is extremely benificial for one who is interested in muscle force activity on articulating joints. These two researchers incorporated 31 muscles into their static model of the lower extremities.

Energy dissipation in my model occurs through viscous damping forces that are assumed to be proportional to joint angular velocity. The coefficeints of proportionality

are defined as joint viscous damping coefficients. While these terms are intended to directly represent viscous effects in joint articulation spaces, they more realistically than probably represent the sum of energy dissipation effects from ligaments and other connective tissues surrounding the joint. They may also include the breaking actions of muscle which occur in the swing leg near the time of heel strike, for example. Impact with the ground at heel strike leads to further kinetic energy losses in addition to the viscous dissipation terms described above. Energy losses from collisions with the ground and at full joint (knee) extension are also included in model calculations.

The force equations for the non-conservative system are presented in chapter 4. In the absence of non-conservative forces, F=0, and these equations of motion in the swing phase reduce to the model of Mochon and McMahon(1), because Mochon and McMahon's model is conservative it cannot be used to compare model solutions of gait in terms of mechanical energy efficiency. Beckett and Chang(8) in their model considered joint moment effects during the swing phase in order to simulate motion which is consistent with geometrical constraints giving minimum energy expenditure. Their work analyzes the motions of the swing leg and foot as well as the equivalent moments occurring in the hip and knee needed to produce motion and energy expenditure of the swing phase of the leg. Since they model only the swing leg possibly important mechanical energy transfers that arise from the coupling between swing and stance leg during walking are not explicitly included. Beckett's model is non-conservative; his study postulates that forces and moments are imposed at the joints of the leg which tends to improve the performance of Mochon and McMahon's model. Using the two postulates of Beckett and Mochon it is postulated in this thesis that by modifying these two principles and using a computer algorithm which computes energy expenditure at heel strike, it is possible to examine this energy loss which should be re-supplied during the double support phase.

2.2 Anthropometric Parameters

To simulate a model of neuromusculoskeletal control of an individual, it is necessary to determine each individual's input parameters. These parameters usually consist of segmental, articular, myodynamic and myocybernetic parameters which relate to the executor (skeletal), myoactuator (muscular) and controller (neural) subsets of the total neuromusculoskeletal system. These three parameter subsets define the neuromusculoskeletal system which could be typically modelled as mass, center of mass and length of segments for the skeletal system, viscous or resistance type elements as well as compliant elements for muscle activity and feedback as a control mechanism in a much more comprehensive model. These parameters consist of upper and lower segments as mentioned above. However, because this model is highly idealized it considers only parameters relating to the lower extremities, with the exception of a lumped parameter to represent upper body mass. Starting parameter values in this model are taken from Dempster's data on normals.

Hatze(11) has done extensive work in prediction of anthropometric values. He found advantages of his model over others because it subdivided segments into small mass elements with differing geometric structures, thus allowing shape and density fluctuations of a segment to be modelled in great detail. His model differentiates between male and female subjects because of exomorphic differences, density function differences, and mass distributions. This is not unusual since females have anatomically different pelvic structure. Hatze's model makes adjustments to densities of certain segmental parts. This process is accomplished by using an indicator located in the region of subcutaneous fat; this also accounts for the specificities of obesity and pregnancy. The procedure is as follows: direct anthropometric measurements are used rather than indirect measurements taken from photo images. This reduces data errors drastically. The reduction of error improves the models overall accuracy better than 3 % with maximum error of 5 %. Hatze experimentally determined parameter values (volumes, center of mass, segmental body

coordinates, moments of inertia) are compared them with model predictions for different subjects.

Wide-spread attention has been given in regard to defining segmental models of the human body, and correctly identifying the morphology of anthropometric segments. Researchers such as: Fisher(12), Hanavan(13), Huston and Passerello(14), and Hatze(11, 15, 16) proposed models each varying in degree of complexity from single, unsegmented rigid body, Hemami(17), to 15 segment models with simple geometric segment shapes as with Hanavan(13). In all cases the models are assumed to be rigid bodies having uniform density. Although very simple models exist, it is generally accepted that more realistic simulations of gross body movement occurs by fragmentation of the body into a minimum of 10 segments (trunk, head, arms, forearms plus hands, thighs, legs plus feet) is essential according to Hatze(11). Figure 2a illustrates segments in a typical walking cycle, most of them were used by Hatze, however, this paper will consider only the lower segments.

It should be noted that over-simplification will introduce additional inconsistencies making the model very inaccurate. These errors are also difficult to detect because they develop mainly in computation of principle moments of inertia and they are not easy to verify.

The overall procedure of Hatze's model is extremely complicated and will be briefly discussed. In general, segments are decomposed into finite-elements of known geometrical structure to obtain volume, mass, coordinates of center of mass and principle moments of inertia. Triple integration of geometrical element boundaries and summation of integrals is basically the method used by Hatze(11) to determine anthropometric parameters by use of a complex mathematical model where he assumes conical and other different geometric shapes to model body segments. His study describes complex algorithms since he considers muscular as well as structural parameters in his model. He examines these anthropometric parameters in great depth with reasonable results obtained.

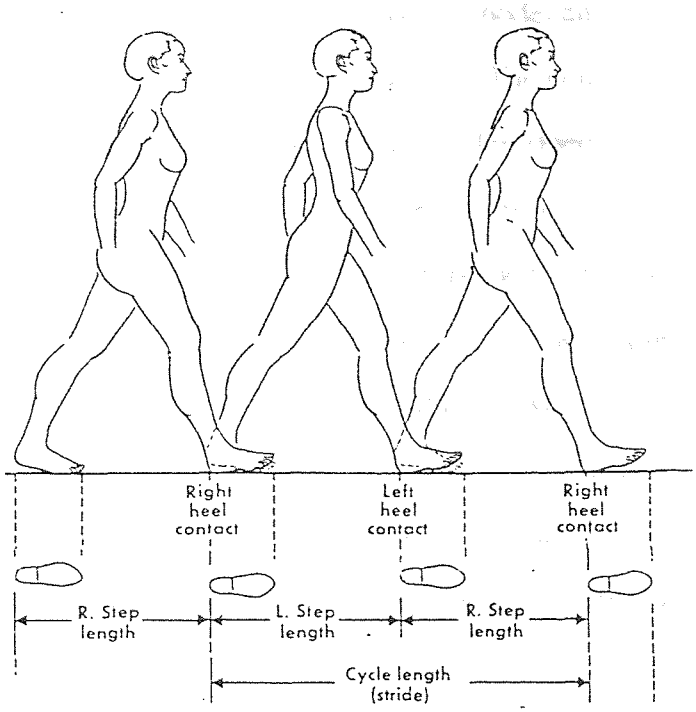

Figure 2a. Typical Walking Cycle.

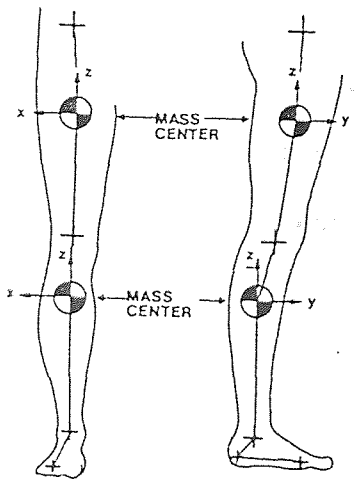

Figure 2b. A lumped mass model of the lower extremities for approximating inertial properties.

The importance of parameter values effects this model and it is likely that because the model is oversimplified, significant error is inevitable. The point is, most models can predict output, and most complex geometries can be described through computer analysis, however, the more segments that are added the better the accuracy of the model.

Hatze(11) described a model using 242 anthropometric measurements a much more complicated model than our study. Model verification with a parameter set as large as Hatze's model is extremely difficult if not impossible. However, his work considered upper extremities such as arms, shoulders and neck, as well as other segments such as the pelvis. It is agreed that pelvic rotation does occur as cited by Inman(3), and that upper body limbs contribute to inertia. Hatze used 17 segments; since we are considering only lower extremities, the model in this study will consist of 3 segments and 11 parameters as listed in appendix A. This is a significant difference, but it is important to note that when considering human motion, the lower extremities is crucial in analysis of gait parameters. The upper body mass can be considered as one lumped mass as well as lower segment masses when approximating inertial properties, as illustrated in figure 2b. These upper body and limbs contribute to the total inertia of the body in motion. With one lumped mass, reasonable results were obtained by Mochon and McMahon(1) and Lacker(6) using this gross simplification of the upper body. Our approach is to gradually increase model complexity starting with simple segment models.

CHAPTER 3

OBJECTIVE

An inverted 3 segment coupled pendulum is, for the most part, rather simplified. Saunders(18) determined from studies of amputees that there are 6 major determinants necessary for human gait, they are: (1) pelvic rotation, (2) pelvic tilt, (3) knee flexion, (4) hip flexion, (5) knee and ankle interaction, and (6) lateral pelvic displacement. They concluded that the loss of any one of these determinants is compensated by the other five, but the loss of two or more will so severely effect human gait that walking may no longer be accomplished. This leads to a premise, suppose determinants (3), (4) and (5) is all that is necessary to permit normal walking, then using this principle the swing leg of human walking can be described by a mathematical model using these three determinants. Most studies of human gait basically focus on the swing phase without considering energy expenditure at the time of heel strike. The swing phase is generally assumed to be the most important phase during the walking cycle because most of the distance achieved in the step length is due to the swing.

The objective is to verify gait model predictions and parameter identification with the objective of ultimately finding optimal solutions by exploring all possible solutions that exist in a solution space. Parameter identification and model validation is very important when considering how well predictions fit with experimental data. If the parameters are changed slightly, output predictions such as angles, velocities and energies are perturbed greatly in some cases that no solution may even exist. This leads to a question: can an optimum walk be achieved in a mathematical model of both swing phase and double support by varying specific gait parameters such as, mass, length of segments, and step length in order to achieve optimum walk by minimizing energy expenditure ? This is the hypothesis that is tested in this paper.

Theoretical predictions will be compared to experimental results to determine if such a model exists and if these results are realizeable. In order to achieve this hypothesis certain guide-lines should be followed for the study of normal or abnormal human gait. They are: (1) the need to address a specific question, formulating a hypothesis and using a method to test that hypothesis. (2) Careful control of inter-dependent gait variables should be maintained, such as walking speed. Inertia and spacial orientation of constantly moving segments change as the walking speed changes. Eksergian's equation given in section 4.1.5, is for kinematic systems and has units of force (Inertia x Acceleration = Force) where inertia is represented by the coefficients also given in section 4.1.5. These coefficients are dependent on angular displacements, when speed changes inertial effects also change. This idea basically explains why speed is important during human walking. The speed of walking greatly influences quantitative measures of most gait variables as illustrated in figures 3a, 3b, and 3c for different segments as reported by Inman(3). These three figures illustrates the effect of changes in speed and hip, knee and ankle displacements for six different subjects during a walk cycle.

Using the principles of Mochon and McMahon(1), that legs move through the swing phase like free swinging pendulums, our model will slightly modify their model since ours considers non-conservative forces, and we will build upon Mochon's model by changing parameters to suit our needs to achieve a model that will hopefully yield reasonable results. The method seems like a guess or way of trying to change something that already works, but we learn from our mistakes and ultimately the goal of obtaining a model with relatively low margin of error can be again modified to yield even better results. Mochon's model is limited in predicting the swing time during normal gait. Their model predicts high speed normal walking with reasonable degree of accuracy, but it only considers the swing phase. If the mechanical energy expenditure during the human walk cycle is to be computed, then Mochon's model cannot be considered because it is conservative; energy must be re-supplied at the double support phase. In this paper the model will modify

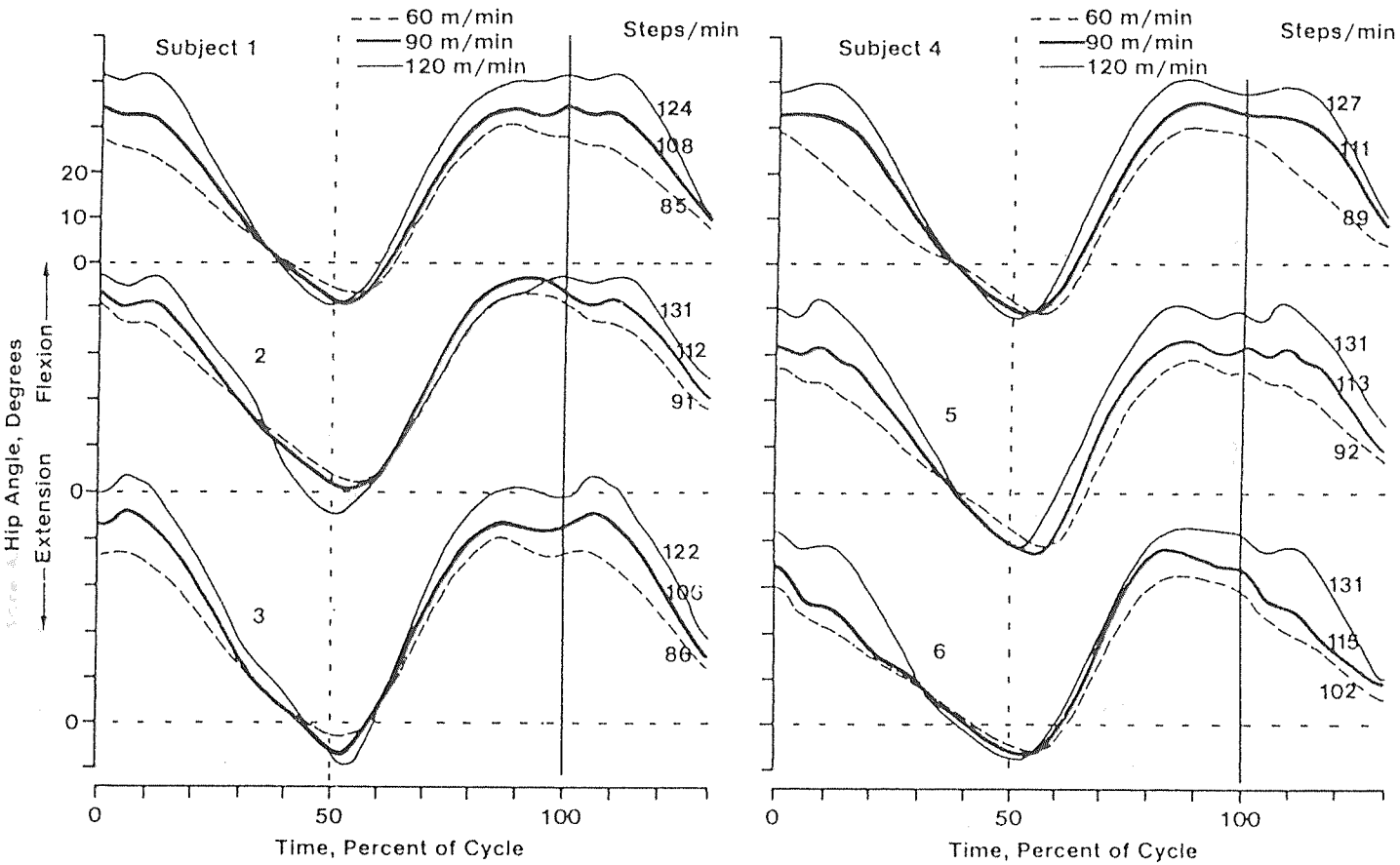

Figure 3a. Effect of speed of walking on hip angle. Six adult male subjects. Speed varied uniformly from 60-120 m/min. Angle at standing position is zero.

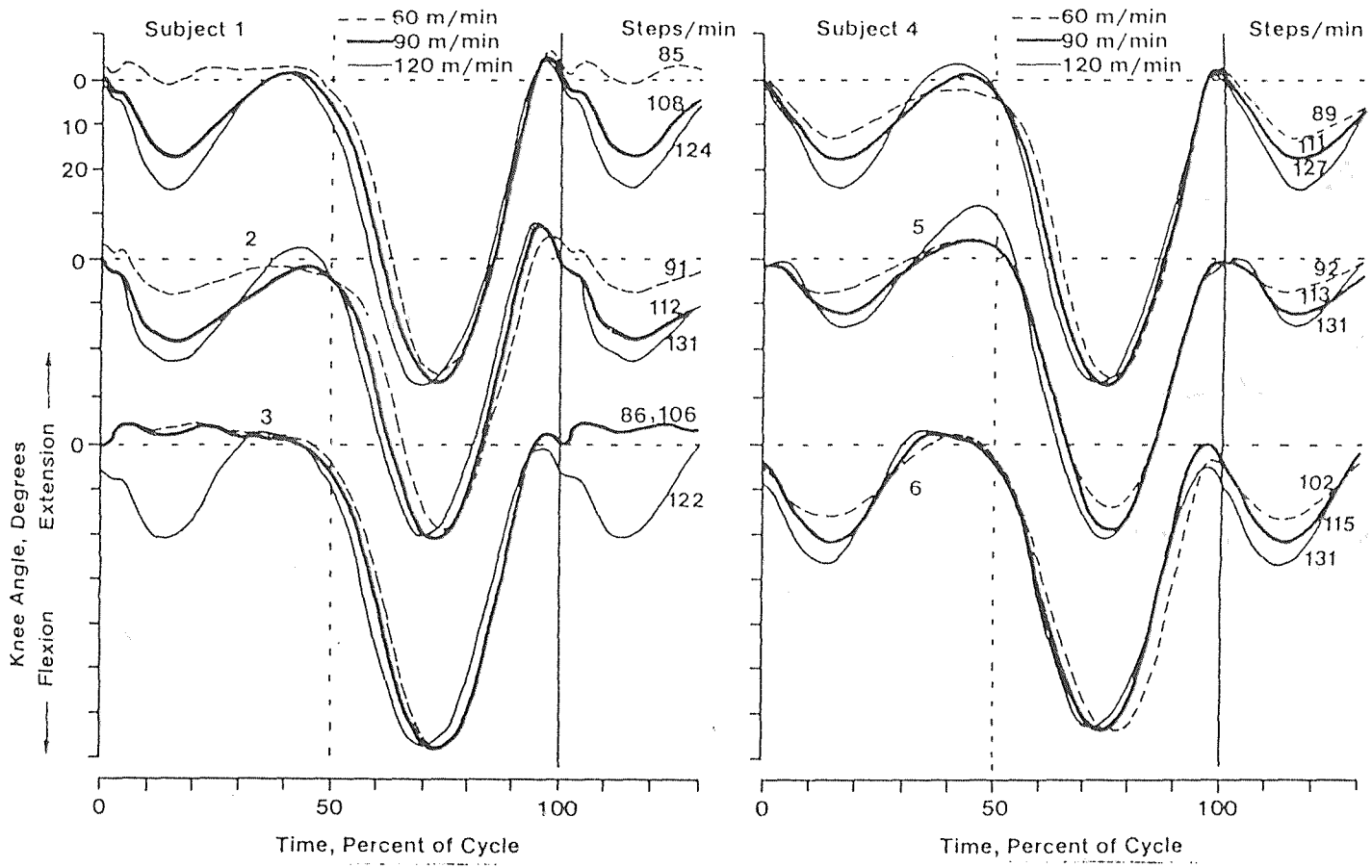

Figure 3b. Effect of speed of walking on knee angle. Six adult male subjects. Speed varied uniformly from 60-120 m/min. Angle at standing position is zero.

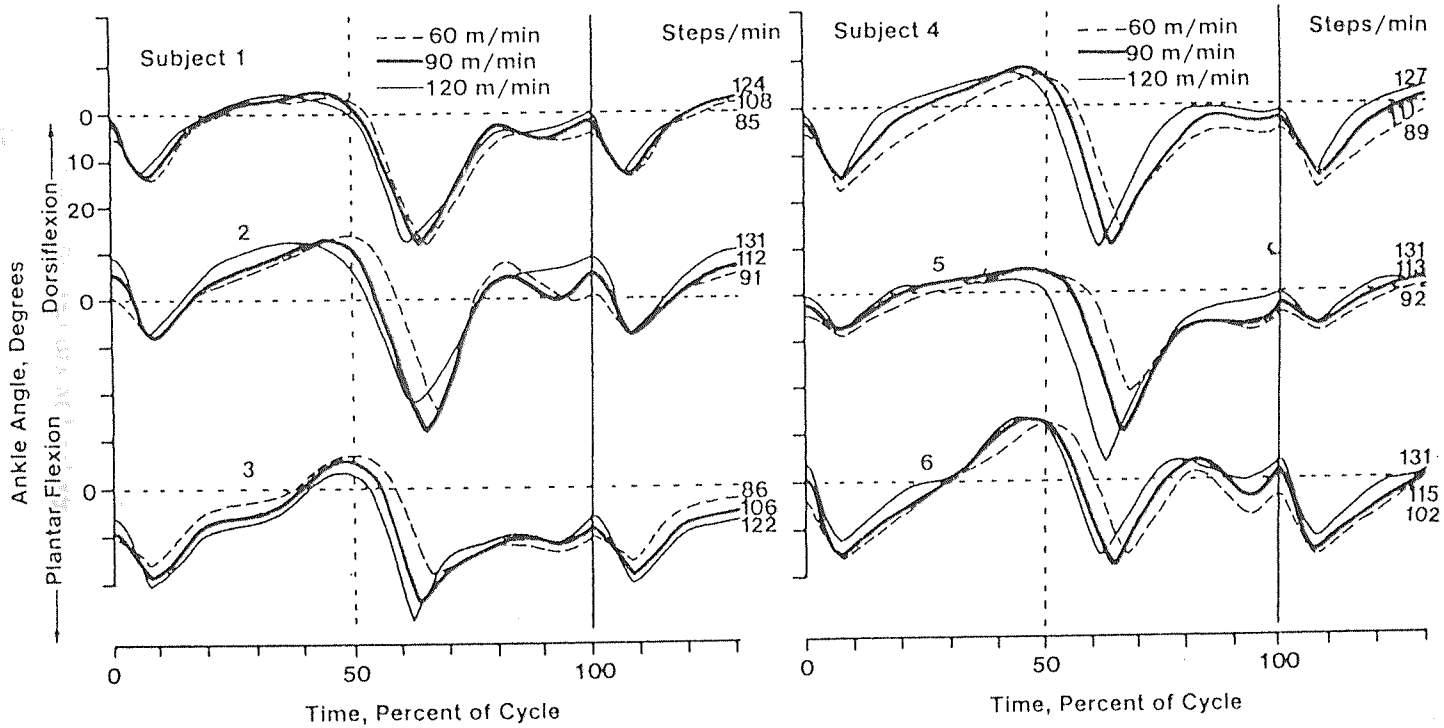

Figure 3c. Effect of speed of walking on ankle angle. Six adult male subjects. Speed varied uniformly from 60-120 m/min. Angle at standing position is zero.

Mochon's assuming the following criteria are met, (1) theoretical results are compared to experimental results by considering articulating joint viscosity which is analogous to resistance of limb motions. (2) By varying gait parameters as well as the swing time we can hopefully obtain a better match to experimental results than with Mochon's model. In the absence of viscosity the coupled pendulum does not really model human walking, rather it is simply a coupled pendulum that can somewhat predict results but has error as with any other model. The error occurs during the swing phase as hyper-extension of the knee occurs and large displacements of the heel are also noticeable. This results in a need to impose a constraint at t = T (time of heel-strike) the angle of the thigh and shank should be kept the same so that $\sigma = \phi$ as shown in fig. 4 at t = T. Ultimately, obtaining a model that will give insight to both the quantitative and qualitative aspects of the swing phase is of importance in regard to using a simple model of a coupled pendulum which models the lower extremities. This model will consider both the effects of gravity and articulating joint viscosity.

Consistent with earlier findings that within a range of walking speeds, muscle forces do not play an active role in the kinetics during the swing phase as with Mochon's. We will investigate the effect of muscle forces during the swing phase incorporated in the viscous dissipation terms to obtain results and compare these results with experimental findings to see if our results are reasonable and if parameter changes are necessary to achieve optimum walk.

The stiff stance leg model, although simplistic, is particularly ideal as a beginning or starting point in any study of human walking because it forms a basis to build upon in future modelling. We have slightly modified Mochon and McMahon's(1) model in order to calculate energy expenditure that occurs at heel strike with the option of varying human gait parameters in order to minimize energy expenditure, therefore, optimizing the walk by reducing energy expenditure. Mochon and McMahon(1) has done further analysis on the effects of additional parameter on human gait. In this paper joint viscosity was added to

the basic model because knee flexion is too large at moderate walking speeds; it is known that knee viscous forces results in less knee flexion during the swing phase. The addition of these velocity dependent joint viscous terms were added to the Lagrange equations in order to improve the qualitative as well as quantitative results, even though the viscous parameters that optimize the best fit with experimental data has not yet been systematically studied in great depth. This model will assume that the energy loss from viscous effects at knee-lock are relatively insignificant, since most of the energy expenditure during the swing phase is the result of impact losses occurring at heel strike. During the walking cycle the mechanical energy that is expended during the swing phase must be restored by muscular effort. The assumption was that muscular effort was restricted to the double support phase, so predictions of mechanical energy can be made of how much muscular effort is necessary to restore energy without knowing such details such as time, length and velocity of active muscle groups.

CHAPTER 4

MATHEMATICAL MODEL

4.1 Equations of Walking Mathematical Model:

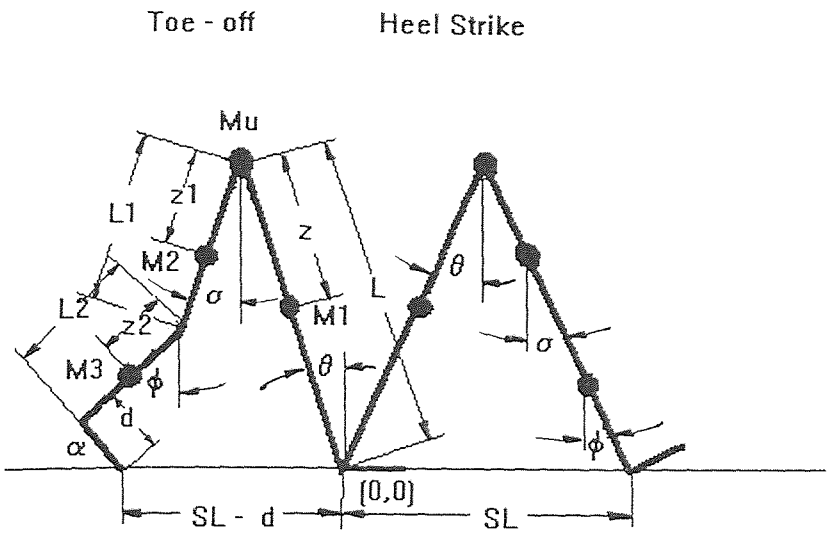

Figure 4 Walking configuration showing toe-off and heel strike. Swing Phase exists between the double support phase. The angles lengths and positions of the center of mass of each limb are shown in the figure. For meaning of symbols see Appendix A. Counterclockwise direction is assumed possitive, clockwise negative.

Equations of Motion:

4.1.1 Position of Center of Mass:

$x_1 = -(L-Z)\sin\theta$ $\qquad$ $y_1 = (L-Z)\cos\theta$

$x_U = -L\sin\theta$ $\qquad$ $y_U = L\cos\theta$

$x_2 = -L\sin\theta + Z_1\sin\sigma$ $\qquad$ $y_2 = L\cos\theta - Z_1\cos\sigma$

$x_3 = -L\sin\theta + L_1\sin\sigma + Z_2\sin\phi$ $\qquad$ $y_3 = L\cos\theta - L_1\cos\sigma - Z_2\cos\phi$

4.1.2 Velocity of Center of Mass:

$\dot{x}_1 = -(L-Z)\cos\theta\dot{\theta}$ $\qquad$ $\dot{y}_1 = -(L-Z)\sin\theta\dot{\theta}$

$\dot{x}_U = -L\cos\theta\dot{\theta}$ $\qquad$ $\dot{y}_U = -L\sin\theta\dot{\theta}$

$\dot{x}_2 = -L\cos\theta\dot{\theta} + Z_1\cos\sigma\dot{\sigma}$ $\qquad$ $\dot{y}_2 = -L\sin\theta\dot{\theta} + Z_1\sin\sigma\dot{\sigma}$

$$\dot{x}_3 = -L\cos\theta\dot{\theta} + L_1\cos\sigma\dot{\sigma} + Z_2\cos\phi\dot{\phi} \qquad \dot{y}_3 = -L\sin\theta\dot{\theta} + L_1\sin\sigma\dot{\sigma} + Z_2\sin\phi\dot{\phi}$$

$$V_1^2 = \dot{x}_1^2 + \dot{y}_1^2 = (L-Z)^2\dot{\theta}^2$$

$$V_U^2 = L^2\dot{\theta}^2$$

$$V_2^2 = \dot{x}_2^2 + \dot{y}_2^2 = L^2\dot{\theta}^2 - 2LZ_1\cos(\theta-\sigma)\dot{\theta}\,\dot{\sigma} + Z_1^2\dot{\sigma}^2$$

$$V_3^2 = \dot{x}_3^2 + \dot{y}_3^2$$

$$= L^2\dot{\theta}^2 - 2LL_1\cos(\theta-\sigma)\dot{\theta}\,\dot{\sigma} + L_1^2\dot{\sigma}^2 - 2LZ_2\cos(\theta-\phi)\dot{\theta}\,\dot{\phi}$$

$$+ 2L_1Z_2\cos(\sigma-\phi)\dot{\sigma}\,\dot{\phi} + Z_2^2\dot{\phi}^2$$

4.1.3 Potential Energy:

$$PE = g(M_1y_1 + M_2y_2 + M_3y_3 + M_Uy_U)$$

$$= g(M_1L - M_1Z + M_UL + M_2L + M_3L)\cos\theta - g(M_2Z_1 + M_3L_1)\cos\sigma - gM_3Z_2\cos\phi$$

$$PE = g(M_TL - M_1Z)\cos\theta - g(M_2Z_1 + M_3L_1)\cos\sigma - gM_3Z_2\cos\phi$$

where the total mass of the system is: $M_T = M_1 + M_2 + M_3 + M_U$

4.1.4 Kinetic Energy:

$$KE = KE_1 + KE_2 + KE_3 + KE_U$$

$$= 1/2\,(M_1V_1^2 + M_2V_2^2 + M_3V_3^2 + M_UV_U^2)$$

$$KE = 1/2\{\,(M_TL^2 - 2M_1LZ + M_1Z^2)\dot{\theta}^2 + (M_2Z_1^2 + M_3L_1^2)\dot{\sigma}^2 + (M_3Z_2^2)\dot{\phi}^2\,\}$$

$$- L(M_2Z_1 + M_3L_1)\cos(\theta-\sigma)\dot{\theta}\,\dot{\sigma} - (M_3LZ_2)\cos(\theta-\phi)\dot{\theta}\,\dot{\phi}$$

$$+ (M_3L_1Z_2)\cos(\sigma-\phi)\dot{\sigma}\,\dot{\phi}$$

4.1.5 Lagrange Equations:

$$L = KE - PE$$

where L is the Lagrangian function for the system. For the generalized non-conservative system the Lagrange equation of motion is:

$$d / dt \left(\partial L / \partial \dot{q}_i \right) - \partial L / \partial q_i = F_i$$

Using generalized coordinates q_i is any generalized body coordinate, $i = 1,2,3,.....,N$

for 3 degree of freedom system this model yields: $q_1 = \theta$, $q_2 = \sigma$, $q_3 = \phi$

For a 3 Segment model: $i = 1,2,3$

with $F_i = 0$ the three Lagrange equations of motion are:

$$d/dt \left(\partial L / \partial \dot{\theta}\right) - \partial L / \partial \theta = 0$$

$$d/dt \left(\partial L / \partial \dot{\sigma}\right) - \partial L / \partial \sigma = 0$$

$$d/dt \left(\partial L / \partial \dot{\phi}\right) - \partial L / \partial \phi = 0$$

Solving these 3 Lagrange equations of motion for the conservative system, we obtain:

$$(M_T L^2 - 2M_1 LZ + M_1 Z^2)\ddot{\theta} - L(M_2 Z_1 + M_3 L_1)\cos(\theta - \sigma)\ddot{\sigma} - (M_3 L Z_2)\cos(\theta - \phi)\ddot{\phi}$$
$$- L(M_2 Z_1 + M_3 L_1)\sin(\theta - \sigma)\dot{\sigma}^2 - (M_3 L Z_2)\sin(\theta - \phi)\dot{\phi}^2 - g(M_T L - M_1 Z)\sin\theta = 0$$

$$- L(M_2 Z_1 + M_3 L_1)\cos(\theta - \sigma)\ddot{\theta} + (M_2 Z_1^2 + M_3 L_1^2)\ddot{\sigma} + (M_3 L_1 Z_2)\cos(\sigma - \phi)\ddot{\phi}$$
$$+ L(M_2 Z_1 + M_3 L_1)\sin(\theta - \sigma)\dot{\theta}^2 + (M_3 L_1 Z_2)\sin(\sigma - \phi)\dot{\phi}^2 + g(M_2 Z_1 + M_3 L_1)\sin\sigma = 0$$

$$- (M_3 L Z_2)\cos(\theta - \phi)\ddot{\theta} + (M_3 L_1 Z_2)\cos(\sigma - \phi)\ddot{\sigma} + M_3 Z_2^2 \ddot{\phi} + (M_3 L Z_2)\sin(\theta - \phi)\dot{\theta}^2$$
$$- (M_3 L_1 Z_2)\sin(\sigma - \phi)\dot{\sigma}^2 + g M_3 Z_2 \sin\phi = 0$$

Lagrange Coefficients needed for Computer Model:

Let, matrix $\{K(q_i)\}$ represent acceleration coefficients, then this matrix has components:

$K_{11} = (M_T L^2 - 2M_1 LZ + M_1 Z^2)$ $\quad$ $K_{12} = -L(M_2 Z_1 + M_3 L_1)\cos(\theta - \sigma)$

$K_{13} = -(M_3 L Z_2)\cos(\theta - \phi)$ $\quad$ $K_{21} = -L(M_2 Z_1 + M_3 L_1)\cos(\theta - \sigma)$

$K_{22} = (M_2 Z_1^2 + M_3 L_1^2)$ $\quad$ $K_{23} = (M_3 L_1 Z_2)\cos(\sigma - \phi)$

$K_{31} = -(M_3 L Z_2)\cos(\theta - \phi)$ $\quad$ $K_{32} = (M_3 L_1 Z_2)\cos(\sigma - \phi)$

$K_{33} = M_3 Z_2^2$

It is obvious from the above equations that: $K_{21} = K_{12}$, $K_{31} = K_{13}$, $K_{32} = K_{23}$

Notice that these coefficients are before accelerations and that their partial deriviatives are before velocity squared terms. These coefficients are represented by a matrix $\{C(qi)\}$. From above the equations, yielding:

$C_{11} = C_{22} = C_{33} = 0$ $\quad$ $C_{21} = -C_{12}$

$C_{12} = -L(M_2 Z_1 + M_3 L_1)\sin(\theta - \sigma)$ $\quad$ $C_{32} = -C_{23}$

$C_{13} = -(M_3 L Z_2)\sin(\theta - \phi)$ $\quad$ $C_{31} = -C_{13}$

These equations are given in the general form as:

$$\{K(q_i)\}\ddot{q}_i + \{C(q_i)\}\dot{q}_i^2 + d(PE)/dq_i = F_i \qquad i = 1,2,3,.....,N$$

and is a form of Eksergian's Kinematic equation(20). The column vector q, is any coordinate variable. The matrix $\{K(q_i)\}$ is symmetric and is the inertia of the system, the matrix $\{C(q_i)\}$ is a skew matrix and is the centripetal component.

When considering the case of an infinite number of segments: $q_i = (\theta, \sigma, \phi \ldots\ldots\infty)$

This model only considers 3 segments, therefore: $i = 1,2,3$ $\quad q = (\theta, \sigma, \phi)$

from the above equation, $\{C(q_i)\}$ is the Jacobian matrix given by:

$$\{C(q_i)\} = \partial \{K(q_i)\}/\partial q_i$$

rewriting we have, $\{K(q_i)\}\ddot{q}_i + (\partial \{K(q_i)\}/\partial q_i)\dot{q}_i^2 + d(PE)/dq_i = F_i$

4.1.6 Dissipative Velocity Dependent Viscous Coefficients:

The model assumes that non-conservative forces are assumed to be due to muscle activity and articulating joint viscosity represented by velocity dependent viscous dissipative coefficients. If muscle forces were assumed not to occur during the swing phase and were restricted to act only during double support then Fi would be due to joint viscosity. Joint viscosity is assumed to be proportional to angular velocity of the joint and acts in directions orthogonal to each of the two limb segments forming the joint angle. The generalized Lagrange equation for the non-conservative system can also be written as:

$$d / dt (\partial L / \partial \dot{q}_i) - \partial L / \partial q_i + \partial D / \partial \dot{q}_i = 0$$

where D is Rayleigh's dissipation function, $D = 1/2 (b_1 \dot{\delta}_1^2 + b_2 \dot{\delta}_2^2 + \ldots\ldots + b_r \dot{\delta}_r^2)$

r = # of viscous dampers

b_i = coefficient of i^{th} viscous damper

$\dot{\delta}_i$ = velocity difference across i^{th} viscous damper ($\dot{\delta}_i$ can be expressed as a function of generalized velocities $\dot{q}_i$)

Considering the 3 degree of freedom system: $i = 1,2,3$

$$D_1 = -1/2\,[b_1\dot{\theta}^2 + b_2(\dot{\theta} - \dot{\sigma})^2]$$

$$\partial D_1/\partial\dot{\theta} = -b_1\dot{\theta} - b_2(\dot{\theta} - \dot{\sigma})$$

$$= -(b_1 + b_2)\dot{\theta} + b_2\dot{\sigma}$$

$$D_2 = 1/2\,[\dot{\sigma}(b_2\dot{\theta} + b_3\dot{\phi}) - (b_2 + b_3)\dot{\sigma}^2 + \dot{\sigma}(b_3\dot{\phi} + b_2\dot{\theta})]$$

$$= 1/2\,[2\dot{\sigma}(b_2\dot{\theta} + b_3\dot{\phi}) - (b_2 + b_3)\dot{\sigma}^2]$$

$$\partial D_2/\partial\dot{\sigma} = (b_2\dot{\theta} + b_3\dot{\phi}) - (b_2 + b_3)\dot{\sigma}$$

$$D_3 = -1/2\,b_3(\dot{\phi} - \dot{\sigma})^2$$

$$\partial D_3/\partial\dot{\phi} = -b_3(\dot{\phi} - \dot{\sigma})$$

Using the idealization that muscle forces do not occur during the swing phase but are restricted to double support, then the non-conservative forces for the 3 segment model is defined as:

$$F_1 = -(b_1 + b_2)\dot{\theta} + b_2\dot{\sigma}$$

$$F_2 = b_2\dot{\theta} - (b_2 + b_3)\dot{\sigma} + b_3\dot{\phi}$$

$$F_3 = b_3\dot{\sigma} - b_3\dot{\phi}$$

Rewriting the equations of motion as they appear in the computer algorithm:

$$K_{11}\ddot{\theta} + K_{12}\ddot{\sigma} + K_{13}\ddot{\phi} + C_{11}\dot{\theta}^2 + C_{12}\dot{\sigma}^2 + C_{13}\dot{\phi}^2 + ga_1\sin\theta = F_1$$
$$K_{21}\ddot{\theta} + K_{22}\ddot{\sigma} + K_{23}\ddot{\phi} + C_{21}\dot{\theta}^2 + C_{22}\dot{\sigma}^2 + C_{23}\dot{\phi}^2 + ga_2\sin\sigma = F_2$$
$$K_{31}\ddot{\theta} + K_{32}\ddot{\sigma} + K_{33}\ddot{\phi} + C_{31}\dot{\theta}^2 + C_{32}\dot{\sigma}^2 + C_{33}\dot{\phi}^2 + ga_3\sin\phi = F_3$$

where: $a_1 = -(M_T L - M_1 Z)$

$a_2 = (M_2 Z_1 + M_3 L_1)$

$a_3 = (M_3 Z_2)$

CHAPTER 5

SOLUTION METHOD

The three Lagrange equations of motion on the bottom of the previous page are solved for the swing phase time T by numerical analysis. A 4th order accurate Runga-Kutta algorithm is used with an initial pair $(q_o,\dot{q}_o)$, where $q_o = (\theta_o, \sigma_o, \phi_o)$ and $\dot{q}_o = (\dot{\theta}_o, \dot{\sigma}_o, \dot{\phi}_o)$ which corresponds to the toe-off configuration at t = 0. The vector q_o is the initial boundary value, the ending configuration occurring at t = T corresponds to the heel strike configuration. In this model T = 0.49 sec approximately for the swing phase time, at this time $q_T = (\theta_T, \sigma_T, \phi_T)$ is determined which is the ending heel strike configuration or second boundary value. In order to solve for q_T the equations at the end of chapter 4 must be solved for accelerations at each time step.

$$\ddot{q}_i\,(t) = (F_i - \{C\,(q_i)\}\dot{q}_i^2 - d(PE)/dq_i) \,/\, \{K(q_i)\} \qquad i = 1,2,3$$

The angular displacements of the walking model throughout the swing phase is completely specified once $q(t) = (\theta(t), \sigma(t), \phi(t))$, $0 \leqslant t \leqslant T$ is determined. The column vector q(t) is uniquely obtained by solving the three Lagrange equations of motion as a two point boundary value problem. In order for a unique solution to be obtained, that being q(t), the initial pair $(q_o, \dot{q}_o)$ must be used to solve the Runga-Kutta iteration scheme. This initial value problem is solved iteratively using the Newton-Raphson method to solve for new initial velocities $\dot{q}_o$. The Newton-Raphson method is shown in figure 5. This new velocity as well as the initial angular displacements qo is used again and again in the Runga-Kutta algorithm until the final boundary point q_T matches the desired ending heel strike configuration. The assumptions that the toe of the swing leg be on the ground at toe-off and that the heel of the swing leg be on the ground at heel strike impose constraints that ultimately determine $\dot{q}_o$ and q_T. These constraints are vertical displacements at toe-off and heel-strike:

$y(to) \geq 0$ Equality at double support, Inequality at swing

$y(hs) \geq 0$ Equality at double support, Inequality at swing

These contraints help determine $(\dot{q}_o, q_T)$ in terms of only two gait parameters, the step length S_L, and the toe-off angle α. The swing leg is assumed to be straight in the knee-lock position at the time of heel strike.

With the parameters given in appendix A, the computer output was determined and theoretical predictions are presented in chapter 7. These results were obtained for the swing phase with the initial toe-off configurations of $q_o = (\theta_o, \sigma_o, \phi_o) = (11.3^\circ, -5.44^\circ, -37^\circ)$ and initial angular velocities $\dot{q}_o = (\dot{\theta}_o, \dot{\sigma}_o, \dot{\phi}_o) = (-71.15^\circ/s, 521.3^\circ/s, -909.85^\circ/s)$.

The purpose of using the Newton-Raphson iteration scheme was to minimize error that occurs at time t = T. Given the initial conditions above, the Runga-Kutta iteration computes $q_T = (\theta_T, \sigma_T, \phi_T)$ with a margin of error, this error is used next in the Newton-Raphson method to solve for new initial velocities $\dot{q}o$ to obtain the desired final boundary point $q_T = (\theta_T, \sigma_T, \phi_T)$ with the least amount of residual error.

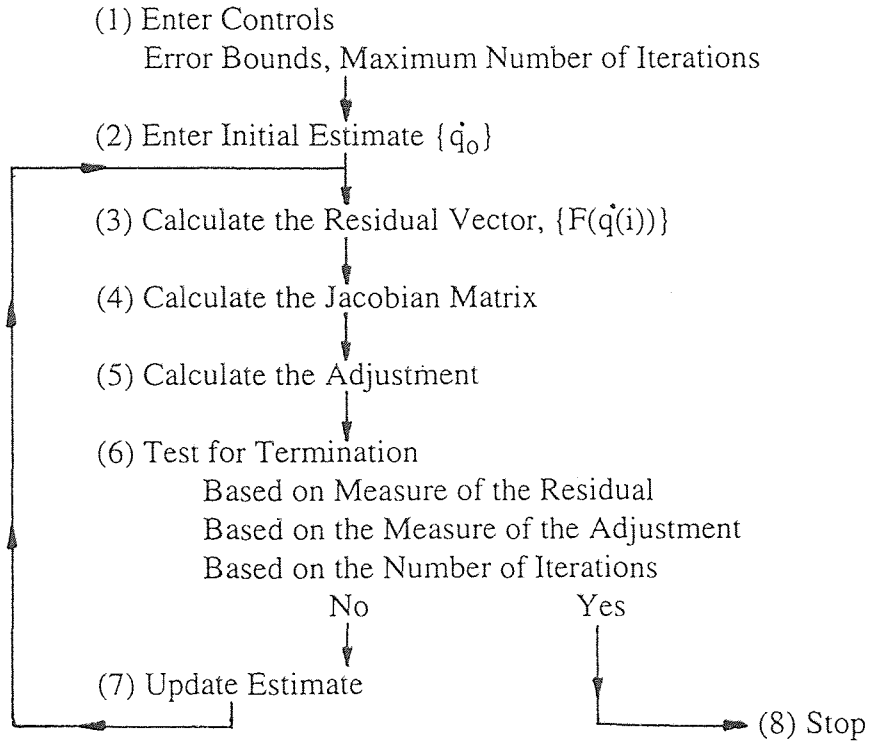

Figure 5. The Newton-Raphson Method

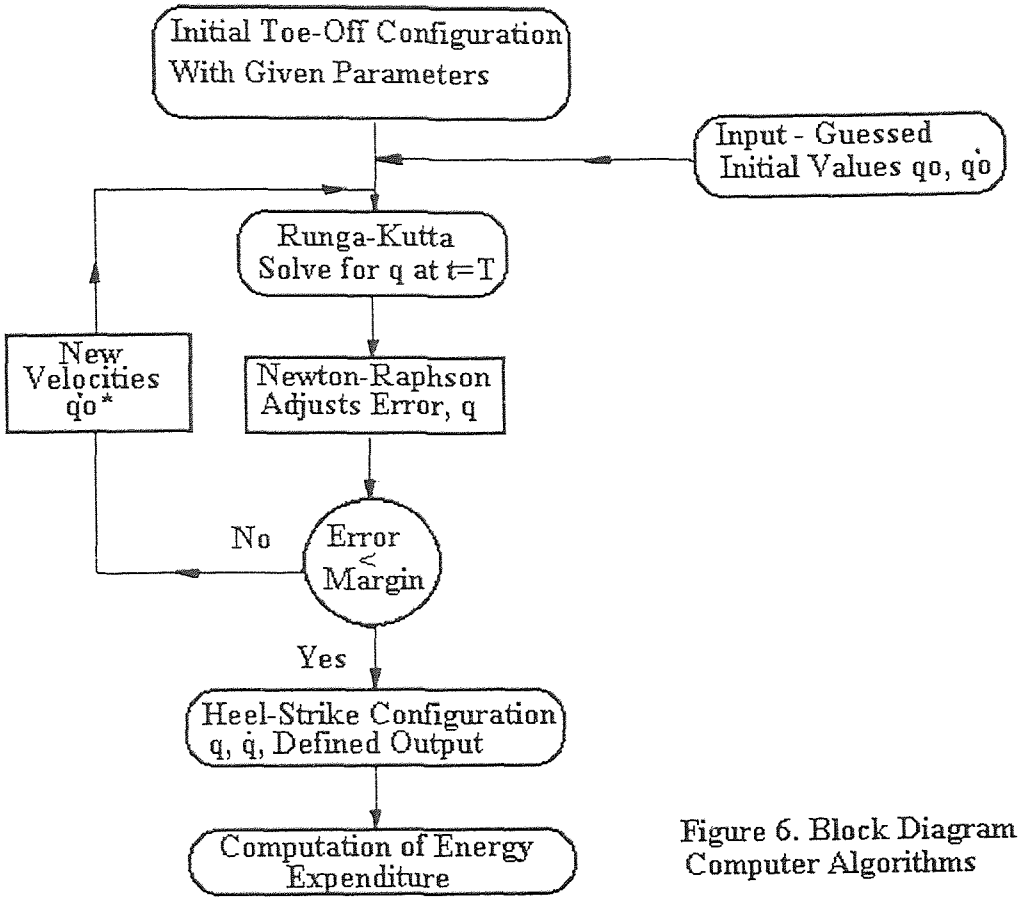

Figure 6. Block Diagram of Computer Algorithms

CHAPTER 6

CALCULATION OF ENERGY LOSSES

6.1 Swing Phase

The solution outlined in chapter 5 is used to determine a unique swing phase gait for walking at a given swing phase speed $v = S_L/T$, with a known step length S_L, and toe-off angle α. This solution uses the pair $(q(t), \dot{q}(t))$, found from Newton's method to calculate the total mechanical energy E(t). This energy is the sum of both potential and kinetic energy of the swing phase so that: $E(t) = \Sigma\,(KE + PE)$, refering to section 4.1.3 and section 4.1.4 the total energy can be written as:

$$E(t) = 1/2\{\ (M_T L^2 - 2M_1 LZ + M_1 Z^2)\dot{\theta}^2 + (M_2 Z_1^{\,2} + M_3 L_1^{\,2})\dot{\sigma}^2 + (M_3 Z_2^{\,2})\dot{\phi}^2\ \}$$
$$- L(M_2 Z_1 + M_3 L_1)\cos(\theta - \sigma)\dot{\theta}\,\dot{\sigma} - (M_3 L Z_2)\cos(\theta - \phi)\dot{\theta}\,\dot{\phi}$$
$$+ (M_3 L_1 Z_2)\cos(\sigma - \phi)\dot{\sigma}\,\dot{\phi} + g(M_T L - M_1 Z)\cos\theta - g(M_2 Z_1 + M_3 L_1)\cos\sigma$$
$$- gM_3 Z_2 \cos\phi$$

In our model, if we assume that muscular effort is restricted to the double support phase, this means that any energy expenditure that occurs during the swing phase will be the result of viscous forces and impact occurring at knee-lock and heel-strike. In most cases these impacts occur almost simultaneously at time T, the end of swing phase. It is understood that these impacts produce discontinuities in the generalized velocity vector $\dot{q}(T)$, as noted by Lacker(10).

6.2 Knee-Lock

If we consider a simple coupled pendulum as acting as the swing leg, then it becomes necessary to impose a physical contraint in order to prevent hyperextension of the knee joint. This physical contraint is refered to as the knee-lock, and it occurs at time $t = T_k$ exactly the time where $\sigma(T_k) = \phi(T_k)$ and $\dot{\phi}(T_k) > \dot{\sigma}(T_k)$. At this point we have only

considered Newton's method from chapter 5 in which a generalized pair $(q(T_k^-), \dot{q}(T_k^-))$ and the energy $E(T_k^-)$ above, both occur just before knee-lock ($t = T_k$). Before this time the velocities of the thigh and shank of the swing leg are moving relative to one another at different velocities but after impact $\dot{\sigma}(T_k^+) = \dot{\phi}(T_k^+)$. These values are necessary in order to prevent hyperextension. Using the principle of momentum conservation which occurs just before knee lock and just after, then $q(T_k^-) = q(T_k^+)$ and $\dot{q}(T_k^+)$ can be found. The momentum of the system is described as $M_i \times V_i$ for any number of segments, in our model i = 1,2,3 so the momentum is given in component form as:

$$M_x = M_1\dot{x}_1 + M_2\dot{x}_2 + M_3\dot{x}_3 + M_U\dot{x}_U \qquad \text{for the x-component}$$

$$M_y = M_1\dot{y}_1 + M_2\dot{y}_2 + M_3\dot{y}_3 + M_U\dot{y}_U \qquad \text{for the y-component}$$

refering to section 4.1.2, this gives:

$$M_x = -M_1(L-Z)\cos\theta\dot{\theta} + M_2(-L\cos\theta\dot{\theta} + Z_1\cos\sigma\dot{\sigma}) + M_3(-L\cos\theta\dot{\theta} + L_1\cos\sigma\dot{\sigma} + Z_2\cos\phi\dot{\phi}) + M_U(-L\cos\theta\dot{\theta})$$

$$* \qquad M_x = (M_1Z - M_TL)\cos\theta\dot{\theta} + (M_2Z_1 + M_3L_1)\cos\sigma\dot{\sigma} + (M_3Z_2)\cos\phi\dot{\phi}$$

$$M_y = -M_1(L-Z)\sin\theta\dot{\theta} + M_2(-L\sin\theta\dot{\theta} + Z_1\sin\sigma\dot{\sigma}) + M_3(-L\sin\theta\dot{\theta} + L_1\sin\sigma\dot{\sigma} + Z_2\sin\phi\dot{\phi}) + M_U(-L\sin\theta\dot{\theta})$$

$$* \qquad M_y = (M_1Z - M_TL)\sin\theta\dot{\theta} + (M_2Z_1 + M_3L_1)\sin\sigma\dot{\sigma} + (M_3Z_2)\sin\phi\dot{\phi}$$

If the principle of energy conservation is to be obeyed then $\dot{q}(T_k^-) = \dot{q}(T_k^+)$, let $\dot{q}(T_k^-) = (\dot{\theta}, \dot{\sigma}, \dot{\phi})$ and $\dot{q}(T_k^+) = (\dot{\theta}^*, \dot{\sigma}^*, \dot{\phi}^*)$ then the x and y components of momentum before and after knee-lock must be the same, by equating these two equalities we obtain:

$$(M_1Z - M_TL)\cos\theta\dot{\theta} + (M_2Z_1 + M_3L_1)\cos\sigma\dot{\sigma} + (M_3Z_2)\cos\phi\dot{\phi}$$
$$= (M_1Z - M_TL)\cos\theta^*\dot{\theta}^* + (M_2Z_1 + M_3L_1)\cos\sigma^*\dot{\sigma}^* + (M_3Z_2)\cos\phi^*\dot{\phi}^*$$

$$(M_1Z - M_TL)\sin\theta\dot{\theta} + (M_2Z_1 + M_3L_1)\sin\sigma\dot{\sigma} + (M_3Z_2)\sin\phi\dot{\phi}$$
$$= (M_1Z - M_TL)\sin\theta^*\dot{\theta}^* + (M_2Z_1 + M_3L_1)\sin\sigma^*\dot{\sigma}^* + (M_3Z_2)\sin\phi^*\dot{\phi}^*$$

Before knee-lock ($\theta, \sigma, \phi, \dot{\theta}, \dot{\sigma}, \dot{\phi}$) are known and also after knee-lock ($\theta = \theta^*, \sigma = \sigma^*, \phi = \phi^*, \sigma^* = \phi^*, \dot{\sigma}^* = \dot{\phi}^*$). Let:

$$P_x = (M_1Z - M_TL)\cos\theta\dot{\theta} + (M_2Z_1 + M_3L_1)\cos\sigma\dot{\sigma} + (M_3Z_2)\cos\phi\dot{\phi}$$
$$P_y = (M_1Z - M_TL)\sin\theta\dot{\theta} + (M_2Z_1 + M_3L_1)\sin\sigma\dot{\sigma} + (M_3Z_2)\sin\phi\dot{\phi}$$

also let: $w_{x1} = (M_1Z - M_TL)\cos\theta^*$ $\quad w_{x2} = (M_2Z_1 + M_3L_1 + M_3Z_2)\cos\sigma^*$

$w_{y1} = (M_1Z - M_TL)\sin\theta^*$ $\quad w_{y2} = (M_2Z_1 + M_3L_1 + M_3Z_2)\sin\sigma^*$

Rewriting these equalities,

$$P_x = w_{x1}\dot{\theta}^* + w_{x2}\dot{\sigma}^*$$
$$P_y = w_{y1}\dot{\theta}^* + w_{y2}\dot{\sigma}^*$$

This linear system is easily solved for the angular velocities of the stance leg, thigh and shank of the swing leg after knee-lock:

$$\dot{\theta}^* = (P_x\, w_{y2} - w_{x2}\, P_y) / (w_{x1}w_{y2} - w_{x2}\, w_{y1})$$
$$\dot{\sigma}^* = (w_{x1}P_y - w_{y1}P_x) / (w_{x1}w_{y2} - w_{x2}\, w_{y1})$$

This unique solution is obtained when the physical constraint $\dot{\sigma}(T_k^+) = \dot{\phi}(T_k^+)$ or $\dot{\sigma}^* = \dot{\phi}^*$ is imposed. Once $\dot{q}(T_k^+)$ is known, $E(T_k^+)$ can be calculated from the energy equation above. The energy loss is $E(T_k^-) - E(T_k^+)$.

6.3 Heel-Strike

At the time of the double support phase the legs reverse their roles in the beginning of a new walking cycle, the previous swing leg is now the new stance leg and the previous stance leg is now the new swing leg as its heel begins to lift off the ground. If we assume

that the position of the heel of the swing leg as it strikes the ground as a new origin for the next step, then the coordinates at the time of heel-strike q(T) become a new set of coordinates ($\theta^*, \sigma^*, \phi^*, \alpha^*$), where, $\theta^*(T) = \sigma(T)$, $\sigma^*(T) = \theta(T)$, $\phi^*(T) = \theta(T)$ and $\alpha^*(T) = 0$. Refering to figure 4, the new coordinate system is shown. During the double support phase just before toe-off, the toe of the new swing leg is on the ground and has position (x_t, y_t), at this time position loop equations can be developed giving:

$$x_t = d - S_L = -L\sin\theta^* + L_1\sin\sigma^* + L_2\sin\phi^* + d\cos\alpha^*$$

$$y_t = 0 = L\cos\theta^* - L_1\cos\sigma^* - L_2\cos\phi^* + d\sin\alpha^*$$

During double support the velocity of the toe is zero, therefore, $(\dot{x}_t = \dot{y}_t = 0)$ and differentiating we obtain:

$$-L\cos\theta^*\dot{\theta}^* + L_1\cos\sigma^*\dot{\sigma}^* + L_2\cos\phi^*\dot{\phi}^* - d\sin\alpha^*\dot{\alpha}^* = 0$$

$$-L\sin\theta^*\dot{\theta}^* + L_1\sin\sigma^*\dot{\sigma}^* + L_2\sin\phi^*\dot{\phi}^* + d\cos\alpha^*\dot{\alpha}^* = 0$$

These equations can be written as:

$$\{v_1, V\} = 0 \qquad \{v_2, V\} = 0$$

where: $V(t) = (\dot{\theta}^*, \dot{\sigma}^*, \dot{\phi}^*, \dot{\alpha}^*)$ is the generalized angular velocity vector.

$$v_1(t) = (-L\cos\theta^*, L_1\cos\sigma^*, L_2\cos\phi^*, -d\sin\alpha^*)$$

$$v_2(t) = (-L\sin\theta^*, L_1\sin\sigma^*, L_2\sin\phi^*, d\cos\alpha^*)$$

These equations express geometrically that the generalized angular velocity vector V(t) throughout the double support phase must lie in a 2-dimensional subspace S and that V(t) is orthogonal to vectors $v_1(t)$ and $v_2(t)$.

In the time before the heel strikes the ground $t = T^-$, the vertical velocity components of the heel does not equal zero, however, just after impact at $t = T^+$ the vertical component must equal zero so as to prevent the foot from going through the floor.

At the end of the swing phase at t = T-, the generalized velocity vector $V(T^-)$ lies outside the subspace S, therefore, at the time of heel-strike impact the generalized

velocity vector $V(T^-)$ must be projected into this subspace S. This projection will produce a new velocity vector at heel-strike $V(T^+)$.

$$V(T^+) = Proj_S V(T^-) = V(T^-) - \{\bar{u}_1, V(T^-)\}\bar{u}_1 - \{\bar{u}_2, V(T^-)\}\bar{u}_2$$

where: $\bar{u}_1 = v_1(T^-) / \|v_1(T^-)\|$

$$\hat{\bar{u}}_2 = v_2(T^-) - \{v_2(T^-), \bar{u}_1\}\bar{u}_1 \qquad \bar{u}_2 = \hat{\bar{u}}_2 / \|\hat{\bar{u}}_2\|$$

are known unit vectors at $t = T^-$. Once this change in angular velocities is known at impact, the change in kinetic energy at heel-strike can be calculated. The potential energy does not change at impact and the energy expenditure can be computed from the energy equation given in section 6.1 so that, $E(T^-) - E(T^+)$ is the energy loss at heel-stike. It should be noted that rigid bodies were assumed in this model for both the limb segments and impact surface, so that no elastic energy is recoverable.

CHAPTER 7

RESULTS

Theoretical predictions for the mathematical model with parameter ratios given by Dempster in Appendix A and initial conditions as discussed in chapter 5 are computed via Runga-Kutta integration and iterative Newton-Raphson error minimizing scheme. Figure 7a. illustrates angular displacements of this particular case, that being model predictions of angles (θ,σ,ϕ) from toe-off to heel-strike.

The two figures 7b. and 7c. represent the non-conservative forces that are attributed to the angular limb velocities and articulating joint viscosity of the hip, knee and ankle. These forces are dissipative with the same assumption as Mochon and McMahon (1), that being the absence of muscle interaction during the swing phase. Figure 7b. illustrates the condition where $b_2 = 0.001$, this viscous dissipative coefficient is acting on the knee joint, similarly figure 7c. illustrates the condition where $b_2 = 0$, note there is only a slight difference in force by adjusting these coefficients, but may be more noticeable at higher velocities due to dissipative effects of the damping coefficients in this particular model.

Energy predictions for this model are also shown in figures 7d. through 7f., it is interesting to note that E(t) is decreasing throughout the swing phase. This energy is restored at heel-strike impact and during the double support phase where there is a translation of potential and kinetic energies. When a new walk cycle begins, E(t) must be restored to initiate the other swing leg that is beginning at the toe-off condition, this process is continuously repeated throughout a walking cycle.

Experimental data is collected by placing reflective markers on anatomical positions, namely the sacrum, left and right anterior superior spine of ilium, articulating knee joint, ankle and toe. Laboratory coordinates are established to determine the true ordinate and abscissa with respect to these markers. Video and computer software (Vicon 370) track these markers in relation to the true ordinate and abscissa and compute relative (x,y,z)

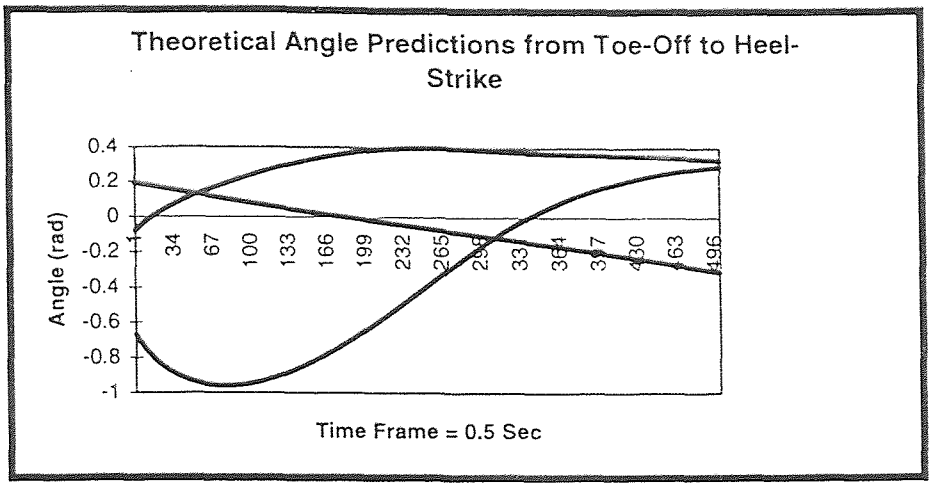

Fig. 7a. Expected Angles: θ = Linear Curve, σ = Upper Curve, ϕ = Lower Curve

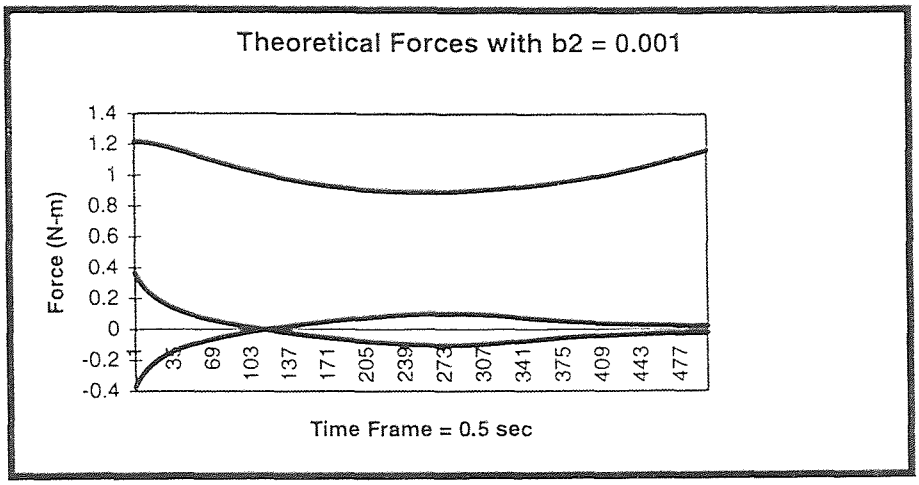

Fig. 7b. Forces with viscous damping at articulating knee. F_1 = Upper Curve, F_2 = Curve that begins negative, F_3 = Curve that begins possitive

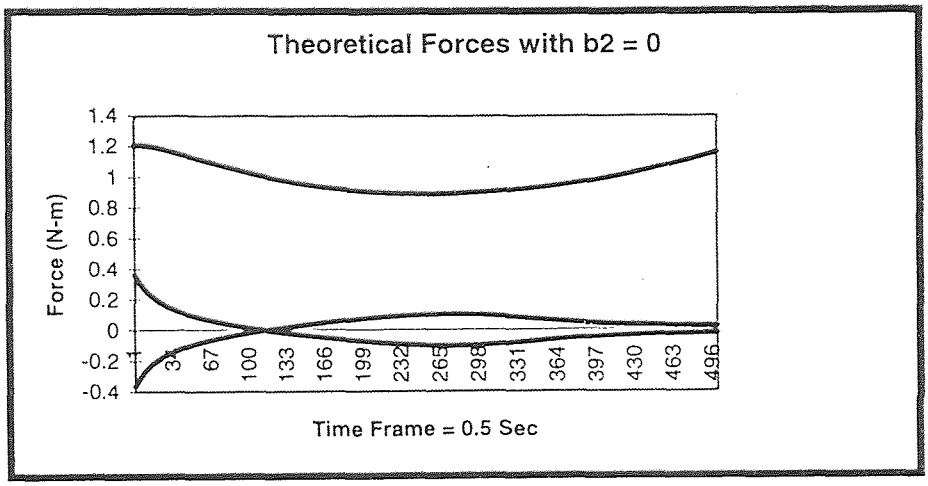

Fig. 7c. Forces without viscous joint viscosity. F_1 = Upper Curve, F_2 = Curve that begins negative, F_3 = Curve that begins possitive

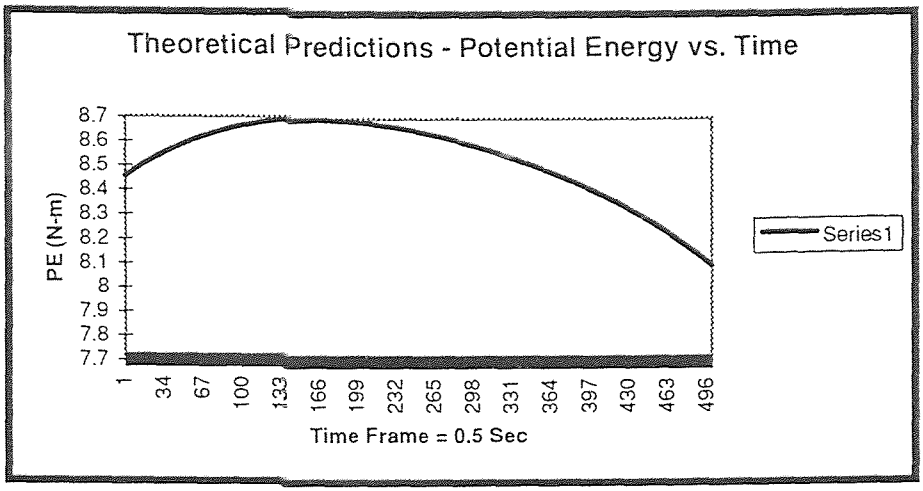

Fig. 7d. Typical Potential Energy Curve

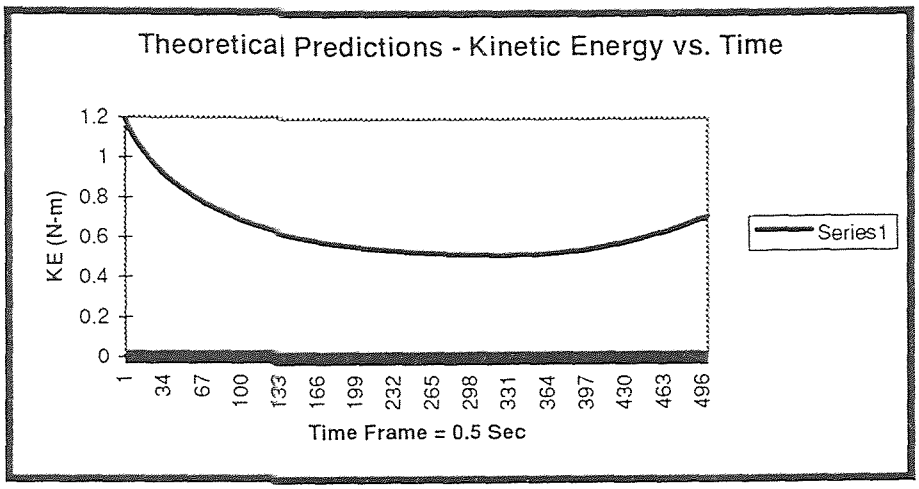

Fig. 7e. Typical Kinetic Energy Curve

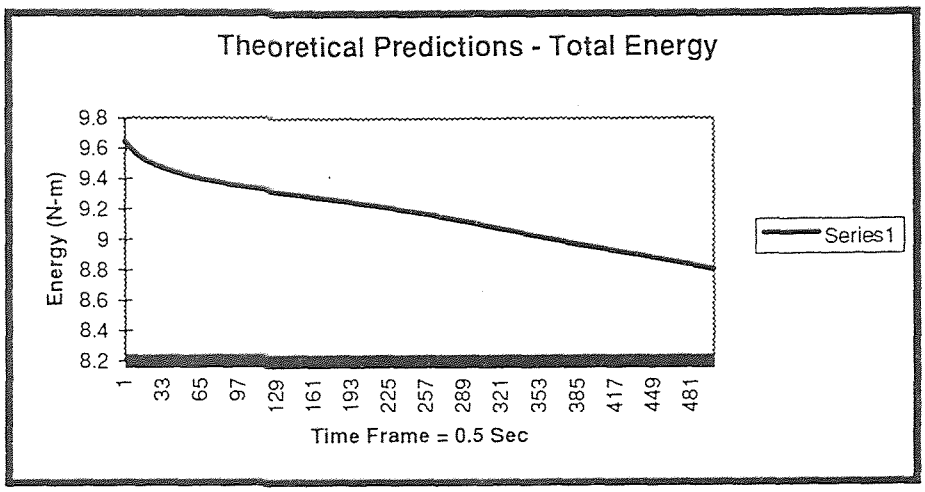

positions. This process yields a three dimensional path of trajectories with respect to the lab coordinates. These (x,y,z) coordinates are calculated during a time frame, each set of coordinates occurs in time at 120 frames / sec .

The experimental data obtained from Vicon 370 motion analyzer is examined for five differing clinical trials as follows:

1) Trial 2 - Normal subjects at prefered walking speed.
2) Trial 5 - 1 lb. weight on right ankle. (Swing Leg)
3) Trial 9 - 2 lb. weight on right ankle. (Swing Leg)
4) Trial 12 - 1lb. weight slightly below right knee. (Swing Leg)
5) Trial 17 - 1 lb. weight on right thigh just above knee. (Swing Leg)

these trials are numbered 2,5,9,12,17 because there was a total of 18 clinical trials and these five were selected in this study. Initially this data was collected from 3-dimensional (x,y,z) rather than 2-dimensional (x,z) coordinates, therefore a projection needed to be applied to this 3-D data onto the sagital plane. The sagital plane is found for each time frame of the experimental record. The process involved bisecting vectors which are defined by (x,y,z) coordinates of the Sac, Lasi, and Rasi as shown in figure 7g.. A vector is defined by two points, using any two points a vector can be found. These points are where markers were positioned at the anatomical positions of the Sac, Lasi, Rasi. The point p(x,y,z) in fig. 7g. was calculated at each increment in time and a bisect vector was then computed.

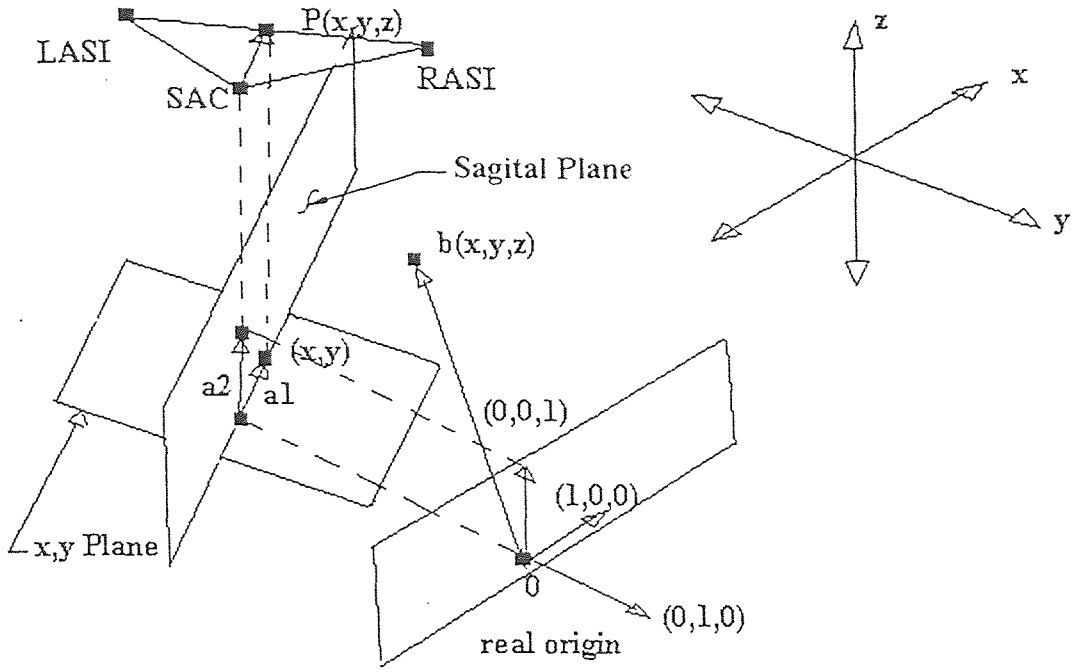

Fig. 7g. Projection theorem for conversion of 3-D data to 2-D.

The theorem is explained as follows:

a1 = the projected bisect vector on the x,y plane

a2 = a unit vector (0,0,1)

A = (a1,a2) is a matrix with basis column vectors a1 and a2

A^T = Transpose of matrix A

b = any other 3-D vector with coordinates (x,y,z) which is to be projected onto the sagital plane.

b_{proj} = the resulting 2-D vector projected onto the sagital plane.

Matrix A has column vectors a1 and a2, these vectors are mutually orthogonal, that is the dot product of these two vectors equals zero. These two vectors are a basis for a plane, therefore matrix A defines the sagital plane.

The sagital plane is calculated at each time frame since a projection has to be calculated to convert 3-D data to 2-D data. Matrix A contains the two basis vectors a1 and a2 which defines the sagital plane and has dimensions (3x2).

A bisect vector is found from the triangular configuration of the Sacrum, Lasi and Rasi as shown in figure 7g., since any two of these three points define a vector, then by using trigonometry we can determine point P(x,y,z). Once this point is determined for each time frame, it is then projected onto the (x,y) plane producing vector a1. Trigonometric calculations are then made with respect to the (x,y) coordinate system to compute angles necessary in determination of the position of the sagital plane. These calculations were made using a computer algorithm. A three dimensional vector b (x,y,z) which can be any marker position with respect to the lab coordinates is then projected onto the sagital plane to produce b_{proj} (x,z), note the y coordinate is omitted because walking is in the x-z direction, y values reflect medial-lateral displacements and are not used in the 2-D model. The projection theorem is defined as follows:

$$b_{proj} = A\,(A^TA)^{-1}\,A^T\,b \qquad \text{where;}\quad (A^TA)^{-1} = (A^TA)_{adjoint} / \text{Det}\,(A^TA)$$

This projected data for each trial was collected and angles were computed for the two dimensional model. The output is shown on page 38.

The addition of the weights in the trials are to see perturbations that develop from the alteration of the inertia effects and changes in the dynamics of the system. This is an important principle involved in testiing the validity of Dempster's parameter values. There exists little, if any, literature available on this subject and the addition of these weights may further enhance current gait studies making them more understandable in regard to what is known of Dempster's parameters.

Projected Data:

Trial 2: Normals w/o weights			Trial 5: 1 lb. Weight on right ankle			Trial 9: 2 lb. Weight on right ankle		
θ	σ	ϕ	θ	σ	ϕ	θ	σ	ϕ
8.3698	-16.99	-46.04	8.0498	-17.66	-36.04	8.77	-17.07	-35.52
7.604	-15.74	-48.04	7.2306	-16.46	-37.15	7.9748	-16.06	-36.48
6.8535	-14.42	-50.22	6.4328	-15.17	-38.05	7.214	-14.83	-37.59
6.0606	-13.08	-52.35	5.6544	-13.7	-38.99	6.4748	-13.51	-38.65
5.1668	-11.67	-54.06	4.8785	-12.45	-39.52	5.7399	-12.4	-39.3
4.3183	-10.17	-55.54	4.0924	-10.72	-40.27	5.0089	-10.88	-40.11
3.5382	-8.629	-56.75	3.3256	-9.089	-40.98	4.3074	-9.784	-40.59
2.7168	-7.066	-57.45	2.5985	-7.775	-40.97	3.5678	-8.679	-40.87
1.8183	-5.525	-57.71	1.868	-6.525	-40.7	2.807	-7.392	-41.1
0.896	-3.957	-57.68	1.0815	-5.243	-40.34	2.0459	-6.143	-40.84
-0.057	-2.414	-57.38	0.3754	-3.977	-40.08	1.4249	-5.239	-40.31
-0.211	-0.923	-56.98	-0.154	-2.682	-39.96	0.9272	-3.974	-40.06
-1.352	0.4993	-56.22	-0.701	-1.363	-39.32	0.3953	-2.92	-39.29
-2.331	1.9618	-55.13	-1.361	-0.101	-38.76	-0.161	-1.888	-38.82
-3.045	3.3733	-53.94	-2.066	1.2784	-38.34	-0.734	-0.786	-38.42
-3.795	4.8056	-52.5	-2.75	2.4791	-37.81	-1.373	0.4101	-37.9
-4.719	6.3205	-50.48	-3.416	3.8092	-37.07	-2.014	1.6524	-37.34
-5.67	7.7348	-48.16	-4.053	5.0397	-36.06	-2.593	2.7259	-36.53
-6.477	9.0795	-45.84	-4.71	5.832	-35.09	-3.203	3.6747	-35.53
-7.168	9.2262	-43.25	-5.377	6.3036	-33.72	-3.829	4.6019	-34.53
-7.819	9.7718	-40.34	-6.021	7.4383	-32.5	-4.448	5.4823	-33.57
-8.495	10.495	-37.39	-6.644	8.3894	-31.2	-5.079	6.2595	-32.65
-9.119	11.305	-34.66	-7.296	9.2167	-29.83	-5.689	7.0144	-31.53
-9.713	12.062	-31.91	-7.39	10.087	-28.33	-6.347	7.7108	-30.17
-10.26	12.697	-28.82	-8.313	10.871	-26.5	-6.684	8.4226	-28.63
-10.81	13.285	-25.57	-9.149	11.593	-25.24	-7.312	9.189	-27.04
-11.35	13.78	-22.38	-9.928	12.252	-23.78	-8.024	10.008	-25.49
-11.88	14.154	-19.18	-10.65	12.853	-21.93	-8.634	10.675	-23.09
-12.4	14.397	-15.71	-11.33	13.443	-19.63	-9.206	11.157	-20.97
-13.05	14.588	-13.29	-11.98	13.816	-16.94	-9.777	11.478	-18.9
-13.66	14.753	-8.253	-12.64	13.896	-14.2	-10.37	11.981	-16.66
-14.29	14.735	-4.357	-13.34	14.047	-11.53	-11.02	12.334	-14.21
-14.92	14.485	-0.483	-14.04	14.404	-8.903	-11.71	12.524	-11.42
-15.86	14.15	3.1536	-14.71	14.325	-5.535	-12.41	12.674	-8.474
-16.64	13.766	6.6584	-15.38	14.103	-2.239	-13.09	12.694	-5.584
-17.23	13.396	10.101	-16.07	14.012	1.1016	-13.73	12.44	-2.468
-17.7	13.125	13.196	-16.79	13.855	4.9677	-14.34	12.094	0.8449
-18.71	12.769	16.141	-17.49	13.334	7.9637	-15.04	11.826	4.1813
-19.54	12.373	18.609	-18.16	12.594	12.865	-15.73	11.447	7.5929
-20.33	12.202	20.269	-18.88	11.961	15.1	-16.36	10.601	10.885
-21.06	12.159	21.161	-19.6	11.679	17.383	-16.97	10.337	13.172
-21.59	12.2	21.484	-20.27	10.849	18.004	-17.62	10.037	15.461
-22.33	12.361	21.257	-20.95	10.791	20.882	-18.32	9.8124	17.395
-22.8	12.54	20.68	-21.7	10.765	21.919	-19.02	9.5793	18.919
-23.08	12.639	19.686	-22.45	11.624	21.609	-19.66	9.4636	19.883
-23.95	12.642	18.334	-23.18	11.396	21.559	-20.32	9.6957	20.214
-24.38	12.631	16.922	-23.84	11.247	21.442	-21.04	10.274	20.009
-25.08	12.599	15.87	-24.51	11.58	20.264	-21.8	9.7828	21.174
			-25.25	12.033	19.266	-22.48	10.301	21.319
						-23.04	10.622	19.352

Table 1: Projected 2-D data obtained from experimental results.

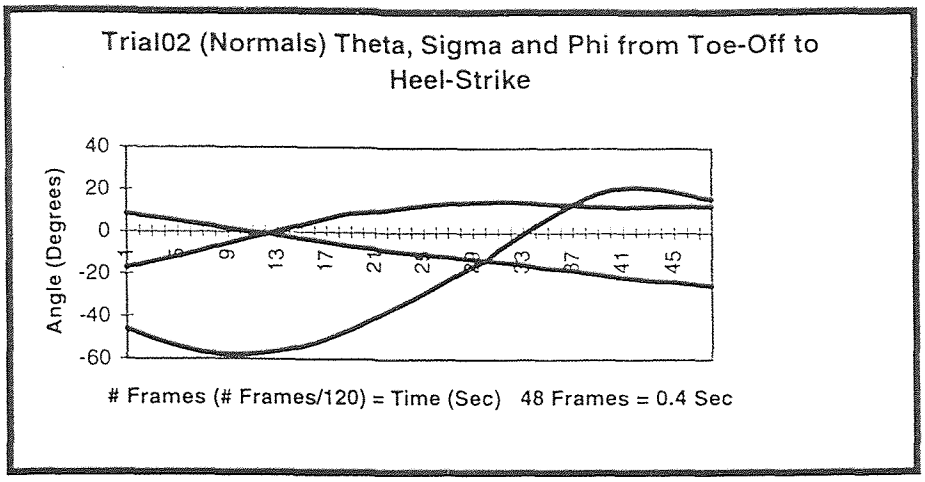

Fig. 8a. Normal Walking - w/o weights.

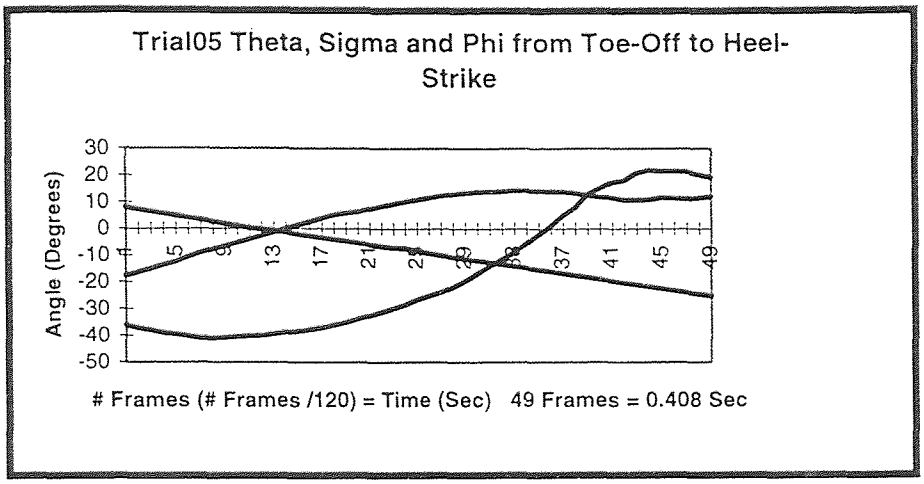

Fig. 8b. 1 lb. Weight on right ankle.

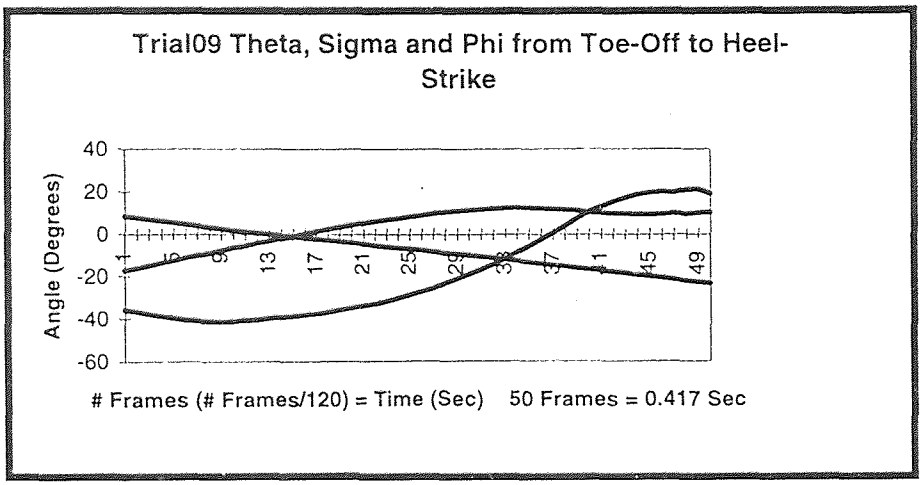

Fig. 8c. 2 lb. Weight on right ankle.

Projected Data:

Trial 12: 1 lb. Weight slightly below right knee			Trial 17: 1 lb. Weight on right thigh just above knee		
θ	σ	ϕ	θ	σ	ϕ
9.5807	-19.6	-33.67	6.7082	-13.87	-38.16
8.7732	-18.7	-34.74	5.8207	-12.73	-38.83
7.9355	-17.59	-35.96	5.0345	-10.88	-40.06
7.0901	-16.46	-37.18	4.2946	-9.618	-40.22
6.3148	-15.36	-38.13	3.4797	-8.039	-40.72
5.6166	-14.06	-38.9	2.6353	-6.518	-41.15
4.9011	-12.8	-39.49	1.8653	-5.113	-41.01
4.1486	-11.55	-39.94	1.2318	-3.711	-40.46
3.3982	-9.972	-40.48	0.6842	-2.405	-40.39
2.6797	-8.398	-40.86	0.1321	-1.174	-39.92
1.9784	-7.111	-40.86	-0.457	0.189	-39.28
1.2304	-5.85	-40.62	-1.129	1.6145	-38.79
0.3966	-4.508	-40.28	-1.812	2.8483	-37.92
-0.292	-3.172	-39.83	-2.49	3.9073	-37.11
-0.687	-1.989	-39.3	-3.217	5.013	-36.25
-1.413	-0.834	-38.7	-3.983	6.1157	-35.21
-2.051	0.2271	-37.91	-4.693	7.1837	-34.07
-2.699	1.2661	-36.9	-5.37	8.3184	-32.9
-3.377	2.4383	-35.94	-6.069	9.076	-31.52
-4.037	3.5575	-34.99	-6.764	10.188	-30.31
-4.705	4.6991	-33.67	-7.469	10.803	-28.84
-5.362	4.9101	-31.42	-7.633	11.611	-26.72
-5.986	6.7214	-30.71	-8.51	11.889	-24.72
-6.623	6.8571	-28.47	-9.349	12.915	-23.25
-7.283	8.291	-27.47	-10.05	13.52	-21.14
-7.986	8.2943	-25.01	-10.67	13.87	-18.7
-8.031	9.9891	-24.17	-11.32	14.313	-16.34
-9.255	10.946	-22.25	-12.04	14.713	-13.86
-9.842	11.558	-20.15	-12.78	14.899	-10.91
-10.54	12.095	-17.7	-13.47	15.021	-8.031
-11.29	12.457	-14.81	-14.12	15.172	-5.018
-12.01	12.805	-11.79	-14.83	15.154	-1.801
-12.71	13.346	-8.799	-15.5	14.945	1.5543
-13.39	13.395	-5.611	-16.21	14.705	4.8072
-14.04	13.36	-2.172	-16.97	14.107	8.2567
-14.75	13.299	1.7292	-17.7	13.62	11.339
-15.48	13.143	5.8471	-18.42	13.187	14.163
-16.16	12.773	8.481	-19.17	12.803	16.805
-16.82	12.328	11.41	-19.96	12.518	18.272
-17.55	12.213	14.257	-20.76	12.342	19.855
-18.27	12.321	16.362	-21.35	12.29	20.243
-18.93	12.226	18.688	-22.15	12.276	20.49
-19.63	11.976	19.365	-22.89	12.005	20.576
-20.42	12.721	18.408	-23.58	11.317	20.583
-21.17	13.396	17.87	-24.17	12.221	19.354
-21.86	13.852	17.604	-24.88	12.742	18.036
-22.54	13.56	16.849	-25.61	12.911	15.931
-23.21	13.421	15.554			
-23.89	13.294	13.923			

Table 2: Projected 2-D data obtained from experimental results.

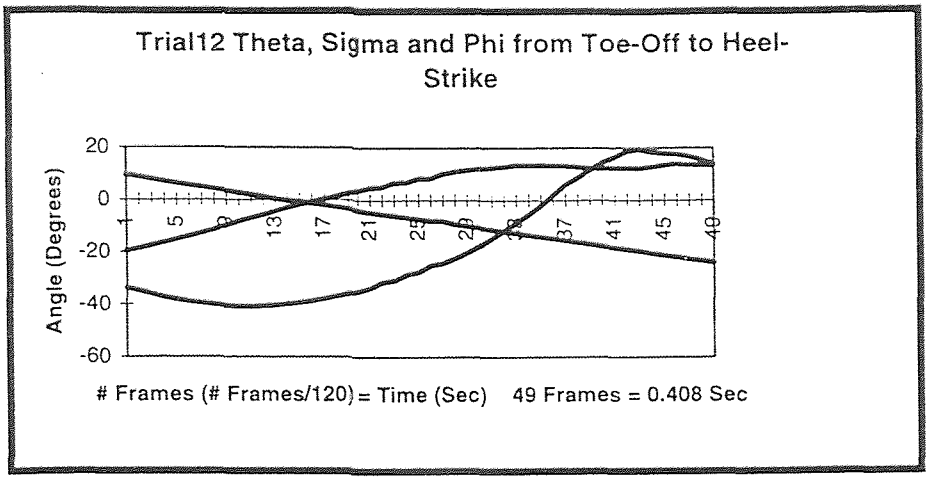

Fig. 8d. 1 lb. Weight slightly below right knee.

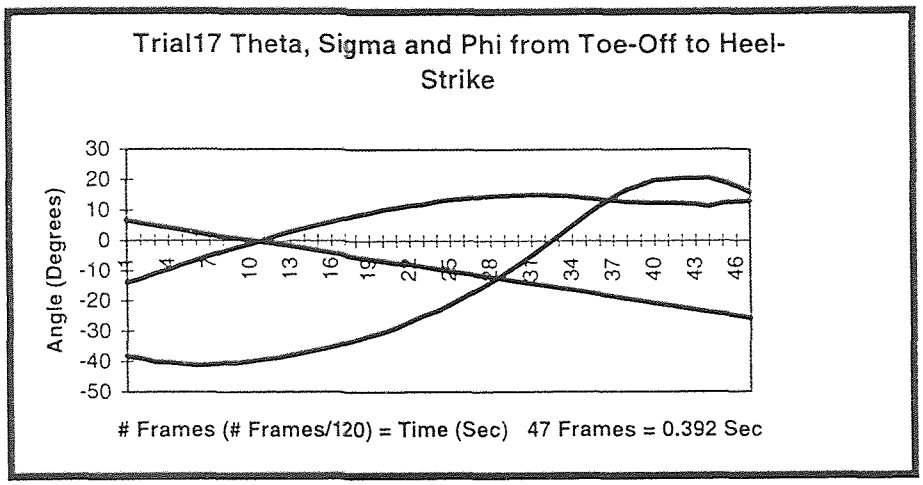

Fig. 8e. 1 lb. Weight on right thigh just above knee.

The goal is to repeat the same numerical procedure as outlined in the model previously except that now by varying gait parameters such as mass. The change in mass may reduce error in model prediction and varify Dempster's data. This is accomplished with an additional numerical procedure known as the downhill simplex method and is discussed in another study.

Projected data with the addition of weights are shown in figures 8a. through 8e. for the five clinical trials outlined above. Note the swing phase time increases by the addition of ankle weights in fig. 8b and 8c. and angular displacements differ slightly in each trial.

When considering parameter identification, such as mass ratios of segments, as defined by Dempster's data can be perturbed in the computer program so that new solutions exist for these different parameter changes, hopefully reducing residuals. Identifying a mass that is needed to satisfy the two point boundary value problem with the subsequent change in Dempster's mass of the model can be examined by the afore mentioned numerical procedures as outlined in Chapt 5 with the addition of the downhill simplex method to further reduce residual error. The change of mass of the segments effects the dynamics of the pendulum as would a change in another parameter such as length. These changes may cause sudden velocity changes resulting in a new region of solution space mainly due to the non-linearity of the equations.

Identifying parameter values is not an easy task, there are many solutions to the 2 point boundary value problem in some cases, other times there exist no solutions in which the model blows-up in extremely large numbers until the computer indicates overflow. The model is sensitive to slight perturbations with mass. The validation of the mathematical model is at this point undetermined since a solution exists that defines all walks in a sub-space with minimum error. The error being discussed is the difference in the desired or target boundary (heel-strike configuration) and the computed value obtained from the mathematical model occurring at time t=T, the end of the swing phase.

Table 3 illustrates the error associated in varying mass of segments in regard to the desired boundary and the computed heel-strike configuration. The additional minimization of error obtained by the downhill simplex method, is not obtainable in this study due to further examination of the solutions already presented.

The validation of the mathematical model in regard to performance has been excellent, model predictions as shown have yielded reasonable results, this present model has also shown excellent results as with Lacker(10). If the validation of the model is to be questioned as far as reliability of theoretical results then the resulting residual error is the primary indicator of model validity, since the goal is to reduce error within reason, usually about 2 %, then the model is as good as what goes into it, if errors are incorporated at the initial computer run, then there is a likelihood that these errors will compile at the end of the run, thus accumulating a greater magnitude of residuals. This present study has errors due to calibration of motion analysis equipment, error due to position of anatomical markers, error due to given model parameter values and error from projected data. There also exists the error associated in the relative simplicity of the model (2-D and three limb segments). These errors compile when combined with one another and result in solutions that often force the shooting method (Newton-Raphson method) to converge to neighboring solutions in a solution space, the downhill simplex method would be the next procedure to minimize these errors even further.

Parameter identification is crucial in order to minimize the error that occurs from the factors mentioned, since the addition of mass is discussed, then identifying new parameter values must be examined by performing iterative Newton's method. This means that computations are performed in order to find new velocities and identification of new mass values and any other parameters in the model that need to be updated to insure minimal error, since the dynamics of the system have been altered. This involves

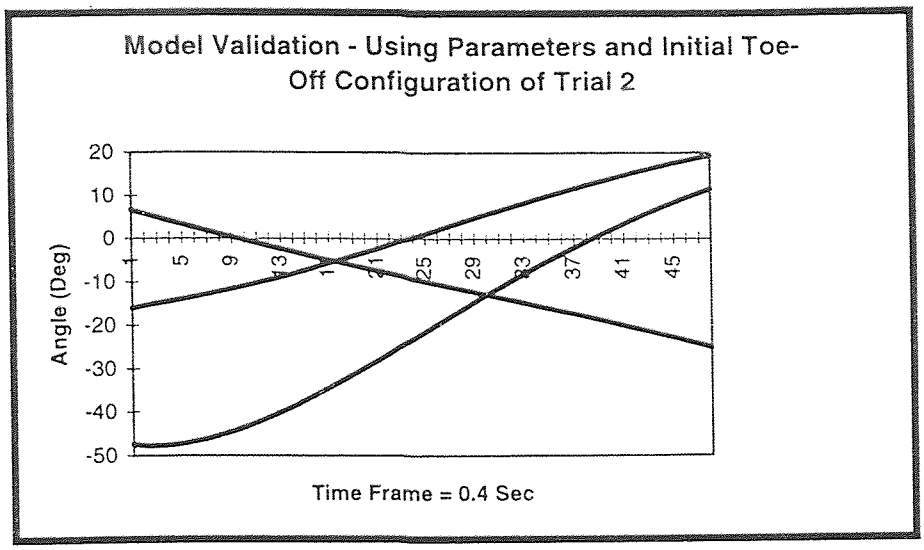

Fig. 8f. Model Validation - Parameters and initial toe-off configuration at the beginning of the swing phase taken from experimental trial 2.

Table 3: Increasing mass to verify Dempster's data.

Trial 5: 1 lb. weight on right ankle of swing leg.

Target: θ_f = - 0.4406 rad σ_f = 0.21 rad ϕ_f = 0.336 rad

Initial Velocity: $\dot{\theta}_o$ = -1.78 rad / sec $\dot{\sigma}_o$ = 1.1 rad / sec $\dot{\phi}_o$ = -3.01 rad / sec

M3	θ_f	σ_f	ϕ_f
0.06 M_T	- 0.438 rad	0.29 rad	0.195 rad
0.07 M_T	- 0.435 rad	0.275 rad	0.202 rad
0.08 M_T	- 0.432 rad	0.264 rad	0.210 rad
0.09 M_T	- 0.428 rad	0.255 rad	0.216 rad

mapping all convergence criteria and finding the least error or best fit of predicted values to experimental values.

Figure 8f. illustrates model validation for trial 2 where no weights were used, note convergence to the desired boundary value. This example used only one of several possible velocities to accomplish the same final configuration as the experimental curve shown in figure 8a. in the same time frame. When considering second order non-linear equations many solutions may exist, this is typical and is represented by the example in figure 8f,. this is only one of many possible valid solutions.

The model can predict within reason and the overall capability of mathematical procedure is important not only in regard to understanding kinematic relationships, but also the numerical computer algorithms needed to solve n equations. The ultimate goal is then in residual error minimization, at this stage computer algorithms are being developed in an effort to accomplish this process. The Newton-Raphson procedure itself is an error minimization technique and is useful, however, it's basic idea relies on error of the magnitude of the residual or the magnitude of the adjustment, it also has strict convergence criteria that may often never be satisfied resulting in possible computer overflow. The validation of the illustrated examples show the model is capable of converging to approximate values, however, the selected parameter values other than length segments need to be modified in order to reduce residuals. The reason lengths do not need to be changed is because these anthropometric parameters are known from experimental static trials.

The velocity obtained by the the mathematical model with the same initial toe-off configuration as that of the experimental trial 2 was computed. This velocity was used in the model validation in order to compare theoretical and experimental results of trial 2, as illustrated in fig 8f., results yield velocities of ($\dot{\theta}_0 = -1.85$ r/sec, $\dot{\sigma}_0 = 1.292$ r/sec, $\dot{\phi}_0 = -2.7$ r/sec). These velocities with known initial toe-off configuration taken from clinical

data, shown at the top of table 1, generate angular displacement curves as shown in fig. 8f. The model is validated by comparing both curves 8a. and 8f., both yield a final heel-strike configuration which are both relatively the same.

The values generated are a solution, however, it is not the only solution and this is important to understand, the error that is associated with this particular case is due to the errors afore mentioned. The results presented so far in this paper correspond to results obtained from Lacker(10), therefore the performance of this model in regard to it's overall validation seems to predict rather well for normal walking speed. These results are varified by Lacker(10) using a similar 2-D model.

CHAPTER 8

DISCUSSION AND CONCLUSIONS

The model that has been shown is an example of the differences in gait with additional weights at each of the three segments of the lower extremities. The model is initially assumed to behave as a simple coupled pendulum system acting under the influence of gravity and joint viscosity. The addition of the non-conservative joint viscosity - velocity dependent coefficients to the Lagrangian equations significantly improves the quantitative and qualitative results even though the viscous parameters that optimize the best fit with existing experimental data has not yet been studied in great detail.

When considering model validity, figure 8f. is absent of additional weights, this figure illustrates a normal walking swing phase cycle for model predictions for the boundary values of trial 2 as shown in chapt. 7. This figure alone shows the validation of the model in regard to solving the two point boundary value problem, since it is a solution and not the only solution the model can therefore be assumed to be valid because the example given in chapter 5 yielded reasonable results, as with Lacker(9).

The addition of the weights changes the gait so that new velocities must develop in order to accomplish a specific swing phase in time, according to the associated two point boundary value problem. This finding is consistent with trial 5, where a 1 lb. weight is secured to the ankle of the swing leg. Each computer solution for trial 5 is listed in table 3 where four different solutions were obtained by increasing the mass M_3 on the ankle segment of the model. Initially the mass that was used was Dempster's data for that mass segment, in this case $M_3 = 0.06\, M_T$. The increase in mass must mean that Dempster's data in the model must be altered in some degree, increasing the mass also means changing centers of mass. Since the model is non-linear, qualitative and quantitative features of the model may be unpredictable. The desired positional boundaries (toe-off

and heel-strike configurations) for trial 5 are shown on table 1, in order to achieve the same toe-off and heel-strike configuration in the same time frame, the model must also be adjusted to achieve this desired heel-strike configuration. The addition of the mass shows in each case that by increasing the ratio of M_3 to M_T the stiff stance leg, L, does not reach the desired position as accurately as in the first case where we used Dempster's data $M_3 = 0.06\ M_T$. This increase in mass tends to decrease the position of the stiff stance leg, however, the swing leg thigh and shank seem to approach the desired position (θ_f, σ_f, ϕ_f) with slightly greater precision. These findings are shown on table 3 where Dempster's data for M_3 was increased from $0.06\ M_T$ to 0.07, 0.08 and $0.09\ M_T$ respectively. The final heel-strike positions are changed somewhat by the addition of the weights, as can be expected. This alone states that the velocity must also change in order to reach the same position in time, this is due to a change in momentum of the coupled pendulum system. The momentum is proportional to the impulse, MV = FT.

Dempster's data on cadavers has been used quite frequently in walking models as with Mochon and McMahon(1) and Lacker(9), however, there has yet been any verification of these gait parameters and very little qualitative information exists in regard to the reliabilty of these parameters in walking models. The output for trial 5 appears to support the possibility that Dempster's data may be in error as much as 15 %. This is not unusual since each individual is structurally different in size and weight that Dempster's data may reflect an average of all possible parameter values.

Parameter values such as mass are not easy to obtain empirically by means of equations, they are measured experimentally by actually finding mass centers from weighing of cadavers. Dempster's data is probably correct for all practical purposes because it has been used previously and is still accepted as a standard. This hoewever,

does not exclude the possibility of these numbers as being incorrect because there is not sufficient data available in order to quantitatively and qualitatively verify these findings.

Examination of the other experimental trials in comparison to theoretical predictions in this study is not necessary since parameter values suggest that Dempster's data is approximate to actual anthropometric parameter values. The experimental curves as shown in figures 8a through 8e identify slight perturbations in angular displacements which may confirm this hypothesis. This slight variation may suggest that Dempster's mass parameters are approximate to the actual mass of cadavers. The length parameters are relatively accurate in determining model predictions, however, the mass can vary significantly as shown by table 3. This does not mean that these values are correct, there exists residual error compiled from several factors as mentioned in chapter 7 and due to the lack of qualitative and quantitative features as mentioned above.

The output presented in table 3 suggests that M_3 may be as much as 0.1 M_T with the addition of the ankle weight. Confirmation of this hypothesis awaits further investigation, this study appears to warrant further examination into the validity of Dempster's data regarding parameter identification. Similar methods to those used in this study attempt to clarify any discrepancies that occur in parameter identification and are used as well as the addition of the downhill simplex method which will be discussed later in another study.

APPENDIX A

Nomenclature

M_T, M_1, M_2, M_3, M_U	Mass of body, leg, thigh, shank, and upper body
L, L_1, L_2	Length of leg, thigh, and shank
Z, Z_1, Z_2	Distance of the center of mass of the leg, thigh, and sha
g	Gravitational constant
S_L	Step length
d	Length of foot
t	Time ranging from $0 < t < T$
T	Swing Phase time
q_i	Generalized coordinate vector $(\theta, \sigma, \phi, ..., \infty)$ $i = 1,2$
θ, σ, ϕ	Angle of leg, thigh and shank w/r to vertical axis (see F
$\dot{\theta}, \dot{\sigma}, \dot{\phi}$	Angular velocities of leg, thigh, and shank
$\ddot{\theta}, \ddot{\sigma}, \ddot{\phi}$	Angular acceleration of leg, thigh and shank
x_1, x_2, x_3	Displacements of x-components center of mass of leg, t and shank w/r to model origin
$y_1, y_2, y_3,$	Displacements of y-components center of mass of leg, t shank w/r to model origin
$\dot{x}_1, \dot{x}_2, \dot{x}_3$	Velocities of x-components center of mass of leg, thigh shank
$\dot{y}_1, \dot{y}_2, \dot{y}_3$	Velocities of y-components center of mass of leg, thigh shank
α	Angle of foot at toe-off w/r to horizontal
b_1, b_2, b_3	Viscous torque coefficients (N-m-s)

Dempster's data on normals as taken from Mochon and McMahon(1)

$M_1/M_T = 0.097$	$M_2/M_T = 0.06$	$M_L = M_1 + M_2$
$L = L_1 + L_2$	$Z_1/L_1 = 0.433$	* $L_1 = L_2$
$Z_2/L_2 = 0.437$	$M_L Z = M_1 Z_1 + M_2 Z_2$	

* This value was changed slightly in this model to: $L_1 = 0.42L$ $L_2 = 0.58L$

Viscous torque values used in this model:

$b_1 = 0.99$

$b_2 = 0$

$b_3 = 0.02$

REFERENCES

(1) Mochon, S., and T.A. McMahon. 1980. "Ballistic Walking." *J. Biomechanics.*13: 49-57

(2) Weber, W., and E. Weber. 1836. *Mechanik der Menschlichen Gehwerkzauge (Mechanics of Human Locomotion).* Göttinger, Gottingen.

(3) Inman, V.T. 1966. "Human Locomotion." *Can. med Ass. J.* 94: 1047-1054

(4) Nubar, Y., and R. Contini. 1961. "A Minimal Principle in Biomechanics." *Bull. math. Biophys.* 23: 377-390

(5) Fenn, W. 1930. "Work against Gravity and Work due to Velocity Changes in Running." *Am. J. Physiol.* 93: 433-462

(6) Fenn, W. 1930. "Frictional and Kinetic Factors in the Work of Sprint Running." *Am. J. Physiol.* 92: 583-611

(7) Seireg, A., and R.J. Arvikar. 1975. "The Prediction of Muscular Load Sharing and Joint Forces in the Lower Extremities during Walking." *J. Biomechanics.* 8: 89-102

(8) Beckett, R., and K. Chang. 1968. "An Evaluation of the Kinematics of Gait by Minimum Energy." *J. Biomechanics.* 1: 147-159

(9) Lacker, H.M. 1993. "A Simple Mathematical Model of the Complete Walking Cycle with Applications to the Physically Disabled." Report No. CAMS-011. Applied Math and Statistics, NJIT

(10) Lacker, H.M. 1993. "Calculation of Mechanical Energy Cost in a Simple Model of Human Walking." Applied Math and Statistics, NJIT

(11) Hatze, H. 1980. "A Mathematical Model for the Computational Determination of Parameter Values of Anthropomorphic Segments." *J. Biomechanics.* 13: 833-843

(12) Fisher, O. 1906. *Theoretische Grundlagen für eine Mechaniik der lebenden Körper.* pp. 52-55, Teubner, Berlin

(13) Hanavan, E.P. 1964. "A Mathematical Model of the Human Body." *Aerospace Med. Res. Lab.* Report No. AMRL-TR-64-102

(14) Huston, R.L., and C.E. Passerello. 1971. "On the Dynamics of Human Body Model." *J. Biomechanics* 4: 369-378

(15) Hatze, H. 1973. Optimization of Human Motions. *In Biomechanics III* (Edited by Cerquiglini, S., A.Venerando, and J. Wartenweiler) pp. 138-142, Karger, Basel.

(16) Hatze, H. 1976. "The Complete Optimization of Human Motion." *Math. Biosci.* 28: 99-135

(17) Hemami, H., and B.F. Wyman. 1979. "Modelling and Control of Constrained Dynamic Systems with Applications to Biped Locomotion in the Frontal Plane." *IEEE Trans. Autom. Control.* AC-24. 4: 526-535

(18) Saunders, J., V.T. Inman, and H.D. Eberhart. 1953. " The Major Determinants in Normal and Pathological Gait." *J. Bone Jt. Surg.* (A) 35: 543-558

(19) Hatze, H. 1981. "A Comprehensive Model for Human Motion Simulation and its Application to the Take-Off Phase of the Long Jump." *J. Biomechanics* 14: 135-142

(20) Doughty, S. 1988. Mechanics of Machines. pp. 256-259